ISSN 1349-1237

SCIENCE REPORTS OF NIIGATA UNIVERSITY

(GEOLOGY)

No. 36 (2021)

Published
by
The Department of Geology, Faculty of Science
Niigata University, Niigata, Japan

31 March 2021

All communications relating to this report should be addressed to:
The editor of
"Science Reports of Niigata University (Geology)"
Department of Geology, Faculty of Science, Niigata University
Niigata 950-2181, Japan

Early Permian (Kungurian) brachiopods from near the base of the Kanokura Formation in the Nagaiwa–Sakamotozawa area, South Kitakami Belt, Japan

Jun-ichi TAZAWA* and Tomohiko SHINTANI**

Abstract

We describe the Tashiroyama brachiopod fauna, consisting of 11 species in 11 genera, from near the base of the Kanokura Formation in the Nagaiwa–Sakamotozawa area, South Kitakami Belt, northeastern Japan. The fauna is of Kungurian age; thus, the lowest part of the Kanokura Formation is correlated with the Kungurian Stage. Palaeobiogeographically, the Tashiroyama fauna is a mixed Boreal–Tethyan fauna, belonging to the Sino-Mongolian–Japanese Province. Thus, South Kitakami, including the Nagaiwa–Sakamotozawa area, was probably located near and to the east of the North China Block during the Kungurian.

Key words: Brachiopoda, Kanokura Formation, Kungurian, Nagaiwa–Sakamotozawa area, South Kitakami Belt.

Introduction

Permian rocks are widely distributed in the South Kitakami Belt, northeastern Japan. The Nagaiwa–Sakamotozawa area in the eastern part of the belt (i.e., Nagaiwa and Sakamotozawa, Hikoroichi-cho, Ofunato City, Iwate Prefecture; Fig. 1B) contains the type locality of the lower Permian Sakamotozawa Formation (named by Onuki, 1937). In this area, the stratigraphy of the Sakamotozawa Formation was studied by Onuki (1937, 1969), Yamada (1959), Kanmera and Mikami (1965a, 1965b), Minato et al. (1979) and Shintani (2011). Recently Ueno et al. (2007, 2009, 2011) described fusulinids from the Sakamotozawa

* Hamaura-cho 1-260-1, Chuo-ku, Niigata 951-8151, Japan
** Dia Consultants Co. Ltd, Toyotsu-cho 5-3, Suita, Osaka 564-0051, Japan
Corresponding author: J. Tazawa,
j1025-tazawa@memoad.jp
(Manuscript received 29 December, 2020; accepted 1 March, 2021)

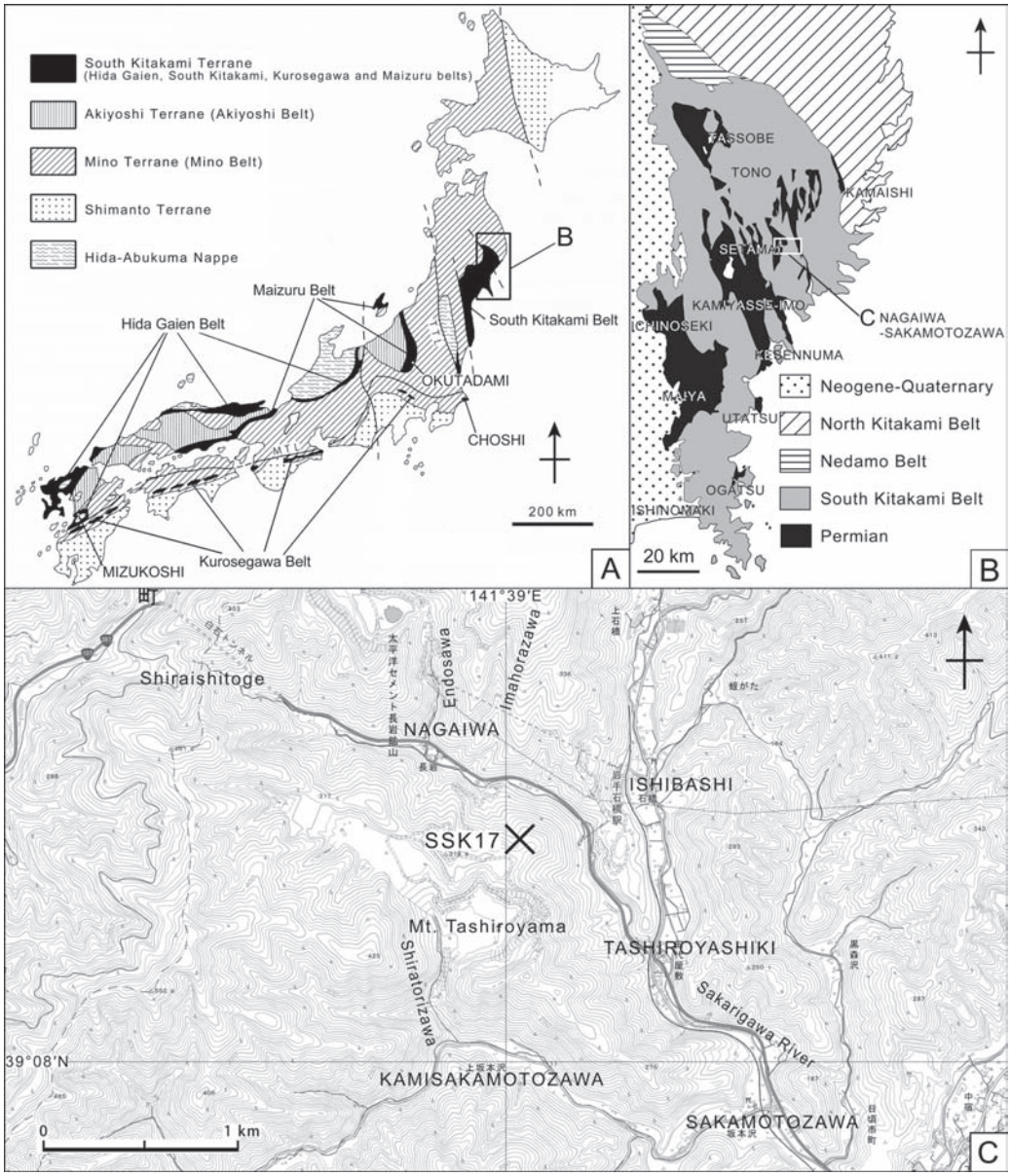

Fig. 1. Maps showing the location and geology of the Nagaiwa–Sakamotozawa area, South Kitakami Belt. (A) Geotectonic map of the Japanese Islands, showing the distribution of the South Kitakami Belt (after Tazawa, 2018); (B) geotectonic map of the northeastern part of Honshu, Japan, showing the distribution of the Permian rocks in the South Kitakami Belt (modified and adapted from Kawamura et al., 2013); and (C) map showing the fossil locality SSK17 at the northern slope of Mt. Tashiroyama in the Nagaiwa–Sakamotozawa area, South Kitakami Belt (using the electronic topographical map of the Geospatial Information Authority of Japan).

Formation, and Tazawa and Shintani (2010, 2015) and Shintani (2011) described brachiopods from the same formation. However, little is known about the stratigraphy, fossil content and age of the overlying Kanokura Formation (named by Onuki, 1937). Kanmera and Mikami

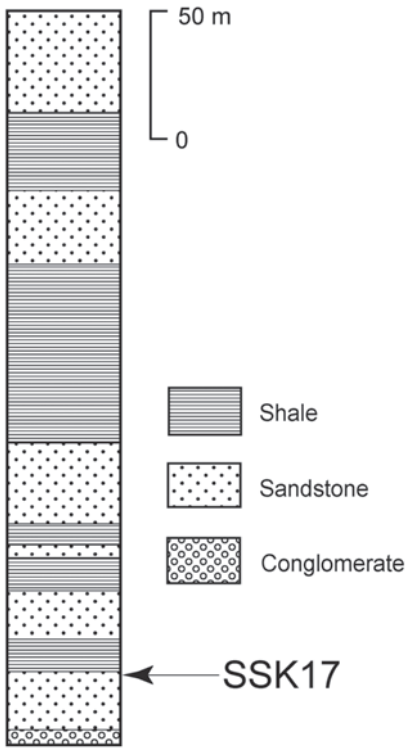

Fig. 2. Generalized columnar section of the Permian Kanokura Formation in the Nagaiwa–Sakamotozawa area, showing the fossil horizon SSK17.

(1965a) studied the stratigraphy of the Kanokura Formation, but did not report any fossils. Therefore, the age of the Kanokura Formatrion in the Nagaiwa–Sakamotozawa area has been uncertain until now.

In the present study, we describe brachiopods from near the base of the Kanokura Formation on the northern slope of Mt. Tashiroyama in the Nagaiwa–Sakamotozawa area, and discuss the age and palaeobiogegraphy of the fossil fauna. The material was collected by T. Shintani in 2006–2007, in the course of his graduate thesis at the Graduate School of Science and Technology, Niigata University, under the supervision of J. Tazawa. The brachiopod specimens described herein are now registered and housed in the Faculty of Science, Niigata University, Niigata (prefix NU-B, numbers 2280–2306).

Stratigraphy and material

In the Nagaiwa–Sakamotozawa area, the Permian strata form the core of a syncline that trends N–S to NNW–SSE and plunges gently towards the north. In this area, the Kanokura Formation (thickness about 460 m) consists mostly of sandstone and shale, with a thin (1–5 m thick) basal conglomerate (Fig. 2). The brachiopod fossils were collected from greenish

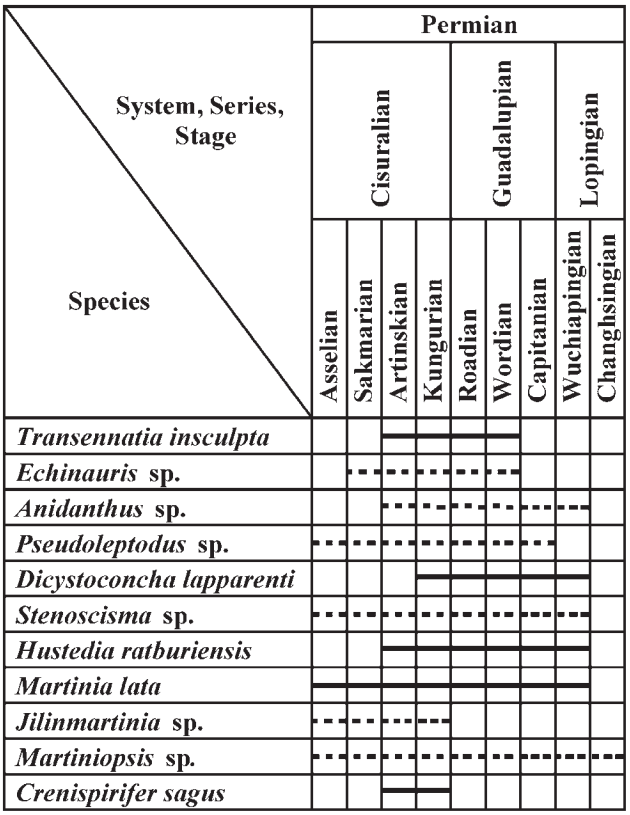

Fig. 3. Stratigraphic distributions of brachiopod species of the Tashiroyama fauna. Broken lines show those of the genera.

grey fine-grained sandstone, 30 m above the base of the Kanokura Formation at locality SSK17 (39°08'36"N, 141°39'04"E; Fig. 1C), 630 m SW of Nagaiwa, northern slope of Mt. Tashiroyama, Kamisakamotozawa, in the Nagaiwa–Sakamotozawa area. The boundary between the Kanokura Formation and the underlying Sakamotozawa Formation is a clinounconformity as reported by Kanmera and Mikami (1965a). Comparing the type section of the Kanokura Formation, described by Tazawa and Ibaraki (2001) in Setamai, about 10 km west of Nagaiwa, the upper part of the formation (consisting mainly of limestone) is lacking in the Nagaiwa–Sakamotozawa area.

The Tashiroyama fauna

The brachiopod fauna described herein includes 11 species in 11 genera: *Transennatia insculpta* (Grant, 1976), *Echinauris* sp., *Anidanthus* sp., *Pseudoleptodus* sp., *Dicystoconcha lapparenti* Termier and Termier in Termier et al., 1974, *Stenoscisma* sp., *Hustedia ratburiensis* Waterhouse and Piyasin, 1970, *Martinia lata* Grabau, 1936, *Jilinmartinia* sp.,

Martiniopsis sp. and *Crenispirifer sagus* Cooper and Grant, 1976b. Of these brachiopods, *Transennatia insculpta* and *Echinauris* sp. are abundant, *Hustedia ratburiensis* and *Martinia lata* are common, and the others are rare.

Age

The stratigraphic distributions of the brachiopod species of the Tashiroyama fauna are summarized in Fig. 3. Of the brachiopod taxa listed above, *Transennatia insculpta* is known from the Artinskian–Wordian (Grant, 1976; Sone in Sone et al., 2003); *Dicystoconcha lapparenti* from the Kungurian–Wuchiapingian (Liang in Wang et al., 1982; Yang, 1984); *Hustedia ratburiensis* from the Artinskian–Wuchiapingian (Archbold, 1999; Tazawa in Tazawa et al., 2015); *Martinia lata* from the Asselian–Wuchiapingian (Grabau, 1936; Tazawa, 2008b); and *Crenispirifer sagus* from the Artinskian–Kungurian (Cooper and Grant, 1976b). At the generic level, *Echinauris* is known from the Sakmarian–Wordian (Brunton et al., 2000); *Anidanthus* from the Artinskian–Wuchiapingian (Brunton et al., 2000); *Pseudoleptodus* from the Asselian–Capitanian (Cooper and Grant, 1974; Grant, 1976); *Stenoscisma* from the lower Carboniferous to the Wuchiapingian (Carlson and Grant, 2002); *Jilinmartinia* from the Moscovian–Kungurian (Pavlova, 1991; Carter and Gourvennec, 2006) and *Martiniopsis* from the upper Carboniferous to the Lopingian (Carter and Gourvennec, 2006). In summary, the Tashiroyama fauna is identified as Kungurian in age; therefore, the lowest part of the Kanokura Formation is correlated with the Kungurian Stage.

Palaeobiogeography

In terms of palaeobiogeography, the Tashiroyama fauna includes both antitropical genera (*Anidanthus* and *Jilinmartinia*) and tropical genera (*Transennatia*, *Echinauris*, *Pseudoleptodus* and *Dicystoconcha*). Therefore, this assemblage represents a mixed Boreal–Tethyan fauna. It is noteworthy that *Jilinmartinia* occurs mostly from northwestern China (Xinjiang) to northeastern China (Jilin). At the species level, *Transennatia insculpta* has been recorded from northwestern China (Xinjiang), southern Thailand and Malaysia; *Dicystoconcha lapparenti* from Afghanistan, northern China (Inner Mongolia), eastern China (Zhejiang) and central-southern China (Hubei and Guangdong); *Hustedia ratburiensis* from central Japan (Hida Gaien Belt), southwestern Japan (Mizukoshi, central Kyushu, western extension of the Hida Gaien Belt), north-central Thailand (Khao Hin King) and southern Thailand (Khao Phrik, Khao Tok Nam and Ko Muk); *Martinia lata* from central-southern China (Guangxi); and *Crenispirifer sagus* from the USA (Texas). To summarize, the Tashiroyama fauna is a mixed Boreal–Tethyan fauna and exhibits affinities with those of northwestern–northeastern China. Thus, the Tashiroyama fauna belonged to the Sino-Mongolian–Japanese Province (of Shi and Tazawa, 2001), which was characterized by the mixture of both Boreal and Tethyan elements and covered the vast area of north and east to the North China Block during the

Permian. South Kitakami, including the Nagaiwa–Sakamotozawa area, was probably located near the North China Block during the Kungurian, in the mid-latitudes of the Northern Hemisphere.

Conclusions

In this study, an early Permian brachiopod fauna (Tashiroyama fauna), consisting of 11 species in 11 genera, is described from near the base of the Kanokura Formation in the Nagaiwa–Sakamotozawa area, South Kitakami Belt, northeastern Japan. The Tashiroyama fauna indicates a Kungurian age. Thus, the lowest part of the Kanokura Formation is correlated with the Kungurian. In terms of palaeobiogeography, the Tashiroyama fauna is a mixed Boreal–Tethyan brachiopod fauna, and has a close affinity with the early Permian brachiopod faunas of northwestern–northeastern China. Thus, the Tashiroyama fauna belonged to the Sino-Mongolian–Japanese Province; and South Kitakami, including the Nagaiwa–Sakamotozawa area, was probably located near and to the east of the North China Block during the Kungurian.

Systematic descriptions

Order Productida Sarytcheva and Sokolskaya, 1959
Suborder Productidina Waagen, 1883
Superfamily Marginiferoidea Stehli, 1954
Family Marginiferidae Stehli, 1954
Subfamily Marginiferinae Stehli, 1954
Genus *Transennatia* Waterhouse, 1975

Type species.—*Productus gratiosus* Waagen, 1884.

Transennatia insculpta (Grant, 1976)
Fig. 4A–C

Gratiosina insculpta Grant, 1976, p. 135, pl. 32, figs. 1–37; pl. 33, figs. 1–16.
Transennatia cf. *insculpta* (Grant). Sone in Sone et al., 2003, p. 528, figs. 7, 8c.
Transennatia insculpta (Grant). Chen, 2004, p. 14, pl. 2, figs. 5–12.

Material.—Six specimens: (1) external and internal moulds of a ventral valve, NU-B2281; (2) external mould of a ventral valve, NU-B2282; (3) external and internal moulds of two dorsal valves, NU-B2283, 2284; (4) external mould of a dorsal valve, NU-B2285; and (5)

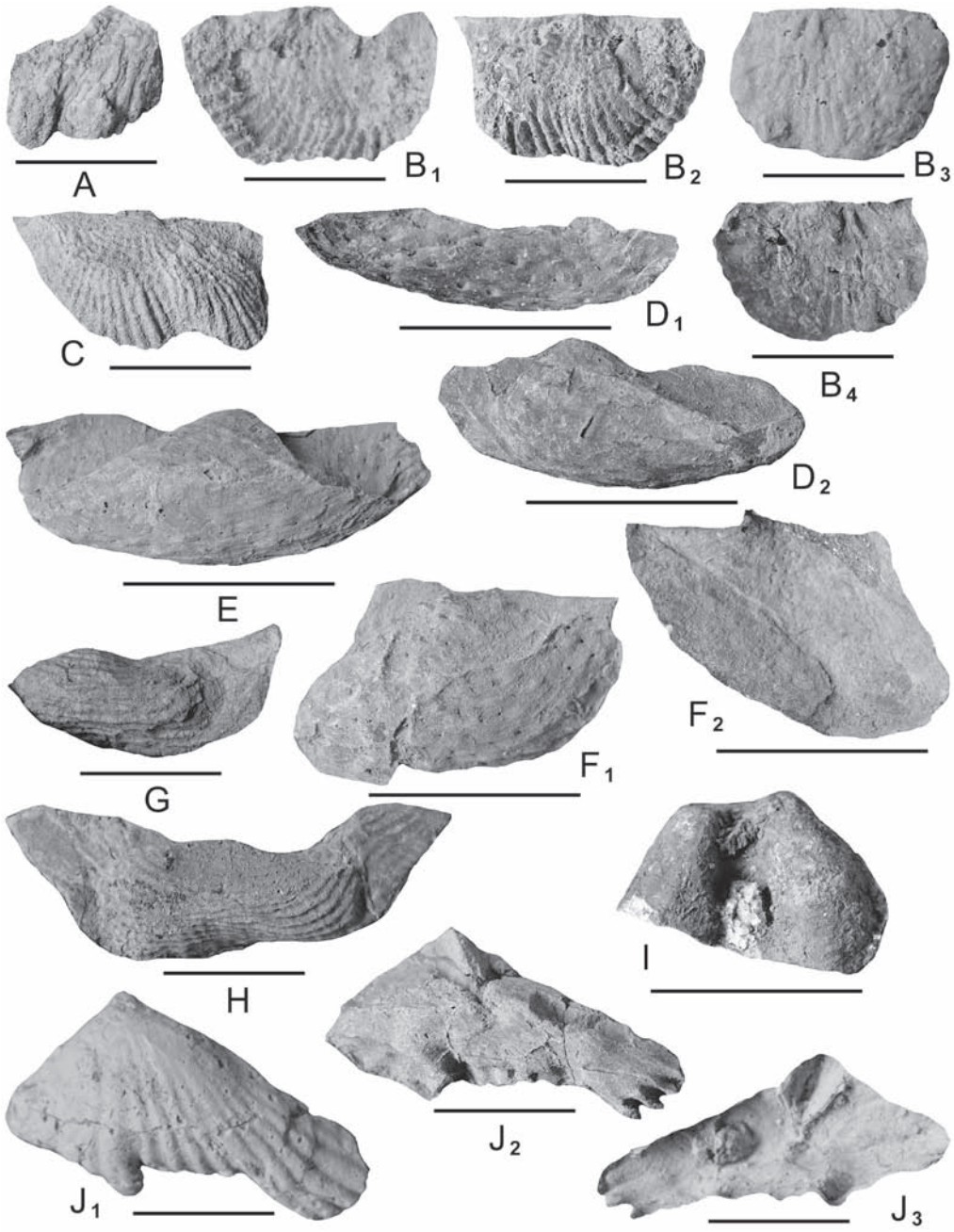

Fig. 4. Brachiopods of the Tashiroyama fauna (1). **A–C**, *Transennatia insculpta* (Grant); A, external latex cast of ventral valve, NU-B2282; external latex cast (B_1), external mould (B_2) and internal latex cast (B_3) of dorsal valve, NU-B2283; C, external mould of dorsal valve, NU-B2284; **D–F**, *Echinauris* sp., external mould (D_1) and internal mould (D_2) of ventral valve, NU-B2287; E, external mould of dorsal valve, NU-B2292; external mould (F_1) and internal mould (F_2) of dorsal valve, NU-B2289; **G**, **H**, *Anidanthus* sp., G, external mould of dorsal valve, NU-B2301; H, external mould of dorsal valve, NU-B2302; **I**, *Dicystoconcha lapparenti* Ternier and Termier; internal mould of ventral valve, NU-B2280; **J**, *Stenoscisma* sp.; external latex cast (J_1), internal mould (J_2) and internal latex cast (J_3) of ventral valve, NU-B2306. Scale bars are 1 cm.

internal mould of a conjoined shell, NU-B2286.

Remarks.—These specimens are referred to *Transennatia insculpta* (Grant, 1976), originally described by Grant (1976, p. 135, pl. 32, figs. 1–37; pl. 33, figs. 1–16) as *Gratiosina insculpta* Grant, 1976, from the Ratburi Formation of Ko Muk, southern Thailand, in the small and transverse shell (length 12 mm, width 19 mm in the best preserved dorsal valve specimen, NU-B2283) and the coarse reticulate ornament on the visceral discs of both ventral and dorsal valves. The type species, *Transennatia gratiosa* (Waagen, 1884, p. 691, pl. 72, figs. 3–7), from the Wargal and Chhidru formations of the Salt Range, Pakistan, differs from *T. insculpta* in the larger size and in having finer reticulate ornament on the discs of both valves.

Distribution.—Artinskian–Wordian: northeastern Japan (Nagaiwa–Sakamotozawa in the South Kitakami Belt), northwestern China (Xinjiang), southern Thailand (Ko Muk) and Malaysia.

Family Costispiniferidae Muir-Wood and Cooper, 1960
Subfamily Costispiniferinae Muir-Wood and Cooper, 1960
Genus *Echinauris* Muir-Wood and Cooper, 1960

Type species.—*Echinauris lateralis* Muir-Wood and Cooper, 1960.

Echinauris sp.
Fig. 4D–F

Material.—Six specimens: (1) external and internal moulds of two ventral valves, NU-B2287, 2288; (2) external and internal moulds of two dorsal valves, NU-B2289, 2290; and (3) external moulds of two dorsal valves, NU-B2291, 2292.

Remarks.—These specimens are safely assigned to the genus *Echinauris* Muir-Wood and Cooper, 1960 by the small, elongate shell (length 11 mm, width 15 mm in the best preserved dorsal valve specimen, NU-B2289), and the external ornaments of numerous stout spine bases on the ventral valve and numerous dimples and fine growth lines on the dorsal valve. The Tashiroyama species is most like *Echinauris crassa* Cooper and Grant (1975, p. 1006, pl. 327, figs. 1–36), from the Leonardian of Texas, the USA, in the transverse outline and in having large ears, but differs from the latter in being wider and larger. *Echinauris interrupta* Cooper and Grant (1975, p. 1006, pl. 328, figs. 1–33), from the Wolfcampian of Texas, differs from the present species in the larger size and in having finer spine bases on the ventral valve. The type species, *Echinauris lateralis* Muir-Wood and Cooper (1960, p. 222, pl. 68, figs. 1–13), from the Word Formation of Texas, is readily distinguished from the present species in the less transverse outline and in having smaller ears. The Tashiroyama species may be a new species of *Echinauris*, although the specimens are poorly preserved.

Superfamily Linoproductoidea Stehli, 1954
Family Linoproductidae Stehli, 1954
Subfamily Anidanthinae Waterhouse, 1968
Genus *Anidanthus* Booker, 1932

Type species.—*Linoproductus springsurensis* Booker, 1932.

Anidanthus sp.
Fig. 4G, H

Material.—Two specimens, external moulds of two dorsal valves, NU-B2301, 2302.

Remarks.—These specimens are safely assigned to the genus *Anidanthus* Booker, 1932 on the basis of lamellose rugae on the visceral disc of the dorsal valve and large, prominent ears with rugae on the valve. *Anidanthus boikowi* (Stepanov, 1946), redescribed by Grigorjeva and Kotlyar (in Sartytcheva, 1977, p. 57, pl. 5, figs. 4–13), from the lower Permian of the Verkhoyansk Range, northern Russia, somewhat resembles the Kitakami species in having large ears but differs in the larger and less transverse dorsal valve. The type species, *Anidanthus springsurensis* (Booker, 1932, p. 67, pl. 3, figs. 1–6; pl. 4, figs. 1–7), from the lower Bowen Series of Queensland, eastern Australia, differs from the present species in being less transverse outline. The Kitakami species is probably a new species, although the material is poorly preserved and not adequate for the establishment.

Suborder Lyttoniidina Williams, Harper and Grant, 2000
Superfamily Lyttonioidea Waagen, 1883
Family Lyttoniidae Waagen, 1883
Subfamily Poikilosakinae Williams, 1953
Genus *Pseudoleptodus* Stehli, 1956

Type species.—*Pseudoleptodus getawayensis* Stehli, 1956.

Pseudoleptodus sp.
Fig. 5A, B

Material.—Two specimens: (1) external and internal moulds of a ventral valve, NU-B2299; and (2) internal mould of a ventral valve, NU-B2300.

Remarks.—The specimens from Mt. Tashiroyama are represented by two incomplete ventral valves lacking the half of lateral sides. They can be assigned to the genus *Pseudoleptodus* Stehli, 1956 in having regularly arranged, low and wide lateral septa, with

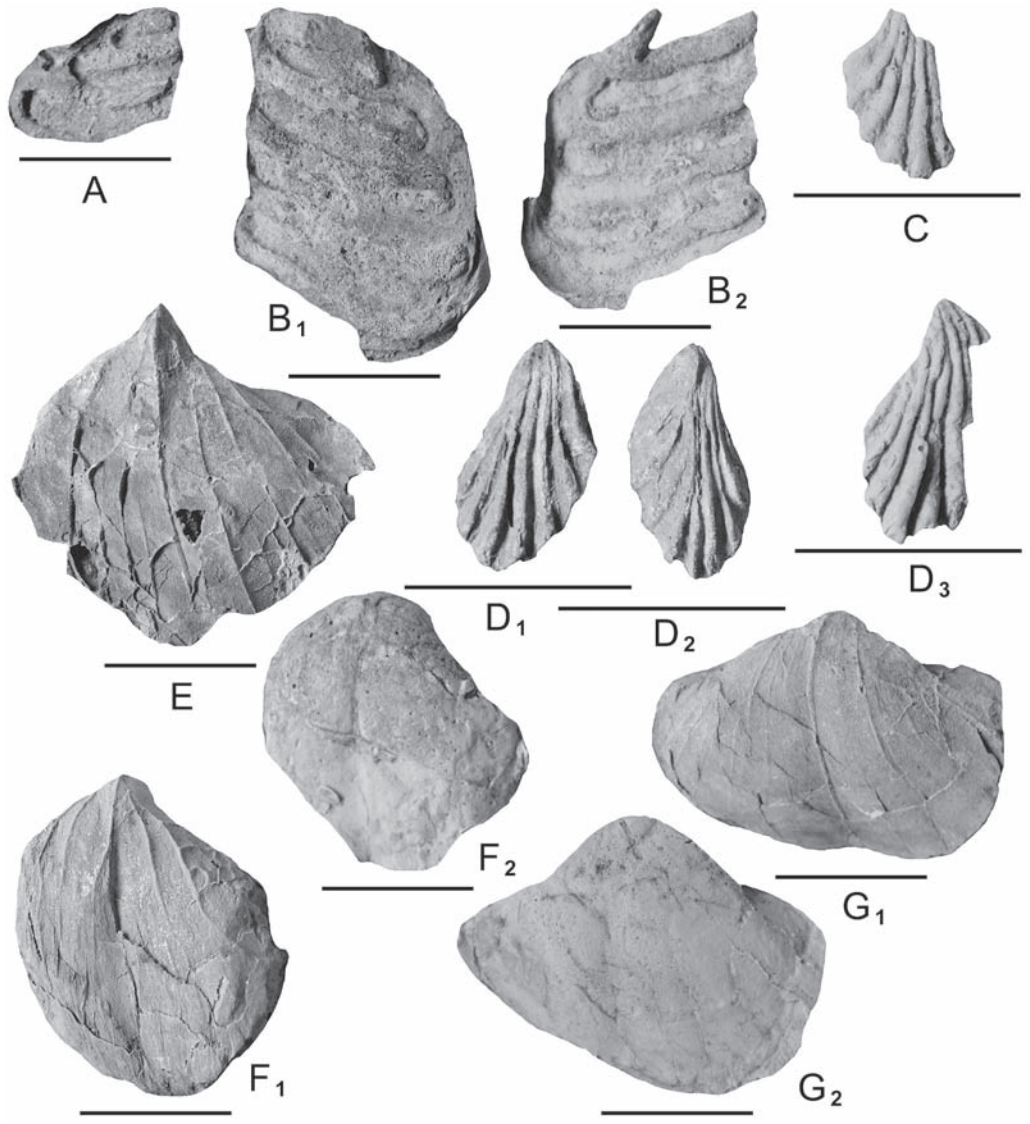

Fig. 5. Brachiopods of the Tashiroyama fauna (2). **A**, **B**, *Pseudoleptodus* sp.; A, internal mould of ventral valve, NU-B2300; internal mould (B_1) and internal latex cast (B_2) of ventral valve, NU-B2299; **C**, **D**, *Hustedia ratburiensis* Waterhouse and Piyasin; C, external latex cast of dorsal valve, NU-B2304; ventral internal mould (D_1), dorsal internal mould (D_2) and dorsal external latex cast (D_3) of conjoined shell, NU-B2303; **E–G**, *Martinia lata* Grabau; E, internal mould of ventral valve, NU-B2295; internal mould (F_1) and external latex cast (F_2) of ventral valve, NU-B2296; internal mould (G_1) and external latex cast (G_2) of ventral valve, NU-B2294; Scale bars are 1 cm.

flattened top. The Kitakami species is probably an advanced-form of the genus, and somewhat resembles *Pseudoleptodus getawayensis* Stehli (1956), redescribed by Cooper and Grant (1974, p. 395, pl. 130, figs. 18–34) from the Cherry Canyon Formation of the Guadalupe

Mountains, Texas, in size and shape of the shell. But the Texan species differs from the Kitakami species in having lateral septa extending anteriorly at steeper angle to the median septum.

Superfamily Permianelloidea He and Zhu, 1979
Family Permianellidae He and Zhu, 1979
Genus *Dicystoconcha* Termier and Termier in Termier et al., 1974

Type species.—*Dicystoconcha lapparenti* Termier and Termier in Termier et al., 1974.

Dicystoconcha lapparenti Termier and Termier in Termier et al., 1974
Fig. 4I

Dicystoconcha lapparenti Termier and Termier in Termier et al., 1974, p. 123, pl. 22, figs. 1, 2, text-fig. 22; Wang and Jin, 1991, p. 495, pl. 1, figs. 1–9; pl. 3, figs. 1–7; Shen and Tazawa, 2014, p. 248, figs. 3.1–3.5; Tazawa et al., 2014, p. 383, fig. 2.6; Tazawa, 2015, p. 73, fig. 6.6; Tazawa and Araki, 2018, p. 16, fig. 4.2.
Dipunctella contricta Liang in Wang et al., 1982, p. 229, pl. 102, fig. 3.
Guangjiayanella guangjiayanensis Yang, 1984, p. 212, pl. 31, figs. 11–16, text-fig. 5.9.
Guangdongina xiamaoensis Mou and Liu, 1989, p. 458, pl. 1, figs. 1–9; pl. 2, figs. 1–7, text-fig. 5.
Guangdongina leguminiformis Mou and Liu, 1989, p. 458, pl. 3, figs. 4–6.
Guangdongina perforates Mou and Liu, 1989, p. 459, pl. 2, fig. 8; pl. 3, figs. 1–3.
Guangdongina sp. Mou and Liu, 1989, p. 459, pl. 2, fig. 9.
Peritisteges latesulcata Liang, 1990, p. 380, pl. 42, figs. 1, 2.
Fabulasteges planata Liang, 1990, p. 381, pl. 42, figs. 3, 4.

Material.—One specimen, internal mould of a ventral valve, NU-B2280.

Remarks.—The single specimen from Mt. Tashiroyama is referred to *Dicystoconcha lapparenti* Termier and Termier (in Termier et al., 1974, p. 123, pl. 22, figs. 1, 2, text-fig. 22), from the lower Murgabian of Wardak, central Afghanistan, in the small, ovate and bilobate ventral valve (length more than 11 mm, width about 13 mm), with shallow incision and a distinct central platform. As discussed by Shen and Tazawa (2014, p. 248), the following six species from the Kungurian–Capitanian of South China are junior synonyms of *Dicystoconcha lapparenti*: *Guangjiayanella guangjiayanensis* Yang, 1984, *Guangdongina xiamaoensis* Mou and Liu, 1989, *G. leguminiformis* Mou and Liu, 1989, *G. perforatus* Mou and Liu, 1989, *Guangdongina* sp. Mou and Liu, 1989 and *Fabulasteges planata* Liang, 1990. Moreover, *Paritisteges latesulcata* Liang (1990, p. 380, pl. 42, figs. 1, 2), from the Wordian of Zhejiang, eastern China, is also considered to be a junior synonym of the present species.

Distribution.—Kungurian–Wuchiapingian: northeastern Japan (Nagaiwa–Sakamotozawa, Kamiyasse–Imo and Hitachi in the South Kitakami Belt), Afghanistan, northern China (Inner Mongolia), eastern China (Zhejiang) and central-southern China (Hubei and Guangdong).

Order Rhynchonellida Kuhn, 1949
Superfamily Stenoscismatoidea Oehlert, 1887
Family Stenoscismatidae Oehlert, 1887
Subfamily Stenoscismatinae Oehlert, 1887
Genus *Stenoscisma* Conrad, 1839

Type species.—*Terebratula schlottheimii* von Buch, 1834.

Stenoscisma sp.
Fig. 4J

Material.—One specimen, external and internal moulds of a ventral valve, NU-B2306.

Remarks.—This specimen is safely assigned to the genus *Stenoscisma* Conrad, 1839 by the rhynchonellid-formed shell, with a spondylium in the ventral valve. The Kitakami species is medium in size (length 15 mm, width 27 mm), transversely subtrigonal in shape, and external surface of the ventral valve is ornamented with strong costae, numbering 4 on sulcus and 5 on each flank. *Stenoscisma hueconianum* (Girty, 1929), redescribed by Cooper and Grant (1976a, p. 2096, pl. 563, figs. 1–54), from the upper Wolfcampian of Texas, resembles the Kitakami species in shape and external ornament of the ventral valve, but differs from the latter in the much smaller size. *Stenoscisma mutabilis* (Tschernyschew, 1902, p. 81, 491, pl. 22, fig. 18; pl. 23, fig. 10; pl. 45, figs. 1–15; pl. 46, fig. 14), from the *Schwagerina* Horizon of the Urals and Timan, resembles the Kitakami species in size, shape and external ornament of the ventral valve, particularly in the medium-sized, transversely subtrigonal specimen (illustrated by Tschernyschew, 1902, pl. 45, fig. 14). However, an accurate comparison is difficult for this poorly preserved specimen.

Order Athyridida Boucot, Johnson and Staton, 1964
Suborder Retziidina Boucot, Johnson and Staton, 1964
Superfamily Retzioidea Waagen, 1883
Family Neoretziidae Dagys, 1972
Subfamily Hustediinae Grunt, 1986
Genus *Hustedia* Hall and Clarke, 1893

Type species.—*Terebratula mormoni* Marcou, 1858.

Hustedia ratburiensis Waterhouse and Piyasin, 1970
Fig. 5C, D

Hustedia ratburiensis Waterhouse and Piyasin, 1970, p. 138, pl. 23, figs. 15–30; Grant, 1976, p. 241, pl. 66, figs. 1–69: pl. 67, figs. 51–58; Yanagida and Nakornsri, 1999, p. 118, pl. 32, figs. 11–16; Archbold, 1999, figs. 5E–H; Tazawa, 2001, p. 299, fig. 8.6; Tazawa, 2008a, p. 53, figs. 8.2–8.6; Tazawa in Tazawa et al., 2015, p. 44, fig. 6.7; Tazawa and Nakamura, 2015, p. 169, figs. 7.1–7.7.
Hustedia nakornsrii Yanagida, 1970, p. 79, pl. 14, fig. 9.

Material.—Three specimens: (1) internal mould of a conjoined shell, with external mould of the dorsal valve, NU-B2303; (2) external mould of a dorsal valve, NU-B2304; and (3) internal mould of a dorsal valve, NU-B2305.

Remarks.—These specimens are referred to *Hustedia ratburiensis* Waterhouse and Piyasin (1970, p. 138, pl. 23, figs. 15–30), from the Wordian of Khao Phrik, southern Thailand, by the medium size (length 11 mm, width 7 mm in the best preserved specimen, NU-B2303) and in having rounded costae which occur three close-set medianly and four pairs laterally on the dorsal valve. *Hustedia nakornsrii* Yanagida (1970, p. 79, pl. 14, fig. 9), from the Ratburi Formation of Khao Phrik, is deemed to be conspecific with the present species. *Hustedia indica* (Waagen, 1883, p. 493, pl. 35, figs. 1, 2), from the Wargal Formation of the Salt Range, differs from *H. ratburiensis* in having fewer and broader costae on both valves.

Distribution.—Artinskian–Wuchiapingian: northeastern Japan (Nagaiwa–Sakamotozawa, Nakadaira and Takakurayama in the South Kitakami Belt), central Japan (Moribu in the Hida Gaien Belt), southwestern Japan (Mizukoshi, central Kyushu, western extension of the Hida Gaien Belt), north-central Thailand (Khao Hin King) and southern Thailand (Khao Phrik, Khao Tok Nam and Ko Muk).

Order Spiriferida Waagen, 1883
Suborder Spiriferidina Waagen, 1883
Superfamily Martinioidea Waagen, 1883
Family Martiniidae Waagen, 1883
Subfamily Martiniinae Waagen, 1883
Genus *Martinia* M'Coy, 1844

Type species.—*Spirifer glaber* Sowerby, 1820.

Martinia lata Grabau, 1936
Fig. 5E–G

Martinia semiplana var. *lata* Grabau, 1936, p. 239, pl. 21, figs. 1–3; Hayasaka and Minato, 1956, p. 146, pl. 23, fig. 3.
Martinia lata Grabau. Tazawa, 2008b, p. 38, figs. 5.7–5.14.

Material.—Three specimens, external and internal moulds of three ventral valves, NU-B2294–2296.

Remarks.—These specimens are referred to *Martinia lata* Grabau, 1936, originally described by Grabau (1936, p. 239, pl. 21, figs. 1–3) as *Martinia semiplana* Waagen var. *lata* Grabau, 1936, from the Maping Formation of Guangxi, central-southern China, by the medium-sized, transversely subelliptical shell (length 17 mm, width 24 mm in the best preserved specimen, NU-B2294) and in having a shallow ventral sulcus. *Martinia semiplana* Waagen (1883, p. 536, pl. 43, fig. 4), from the Wargal Formation of the Salt Range, differs from *M. lata* in the smaller size and less transverse outline.

Distribution.—Asselian–Wuchiapingian: northeastern Japan (Nagaiwa–Sakamotozawa, Kamiyasse–Imo and Takakurayama in the South Kitakami Belt) and central-southern China (Guangxi).

Genus *Jilinmartinia* Lee and Gu, 1980

Type species.—*Brachythyris shansiensis* Chao, 1929.

Jilinmartinia sp.
Fig. 6C

Material.—One specimen, external and internal moulds of a conjoined shell, NU-B2293.

Remarks.—The single specimen from Mt. Tashiroyama is safely assigned to the genus *Jilinmartinia* Lee and Gu, 1980 by the large size (length about 33 mm, width about 85 mm), wider subcircular outline, moderately developed sulcus, external ornament consisting of fine concentric growth lines, and some radial vascular markings in the ventral valve. The Kitakami species resembles the type species, *Jilinmartinia shansiensis* (Chao, 1929), originally described by Chao (1929, p. 55, pl. 9, figs. 1–3) as *Brachythyris shansiensis* Chao, 1929, from the Lichiachuan Formation (Asselian) of Gansu, northwestern China, in size and shape of the shell and external ornament of the ventral valve. But the Chinese species differs from the present species in the less transverse outline and in having narrower and deeper sulcus on the ventral valve. *Jilinmartinia sokolovi* (Tschernyschew, 1902, p. 166, pl. 8, fig. 3; pl. 39, fig.

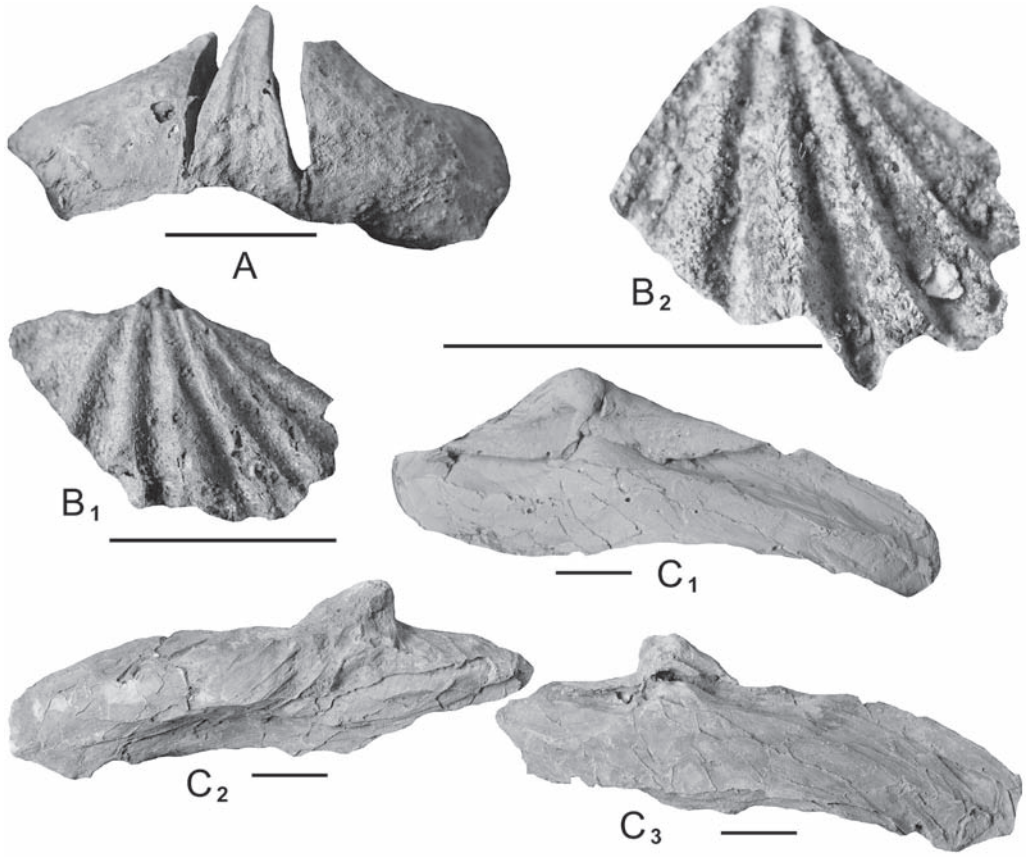

Fig. 6. Brachiopods of the Tashiroyama fauna (3). **A**, *Martiniopsis* sp., internal mould of ventral valve, NU-B2297; **B**, *Crenispirifer sagus* Cooper and Grant; internal mould (B_1) and external latex cast (B_2) of dorsal valve, NU-B2298; **C**, *Jilinmartinia* sp.; dorsal external latex cast (C_1), ventral internal mould (C_2) and dorsal internal mould (C_3) of conjoined shell, NU-B2293. Scale bars are 1 cm.

4), from the Asselian of the Urals, is also a transverse *Jilinmartinia* species, but the Russian species differs from the Kitakami species in having two costae in the ventral sulcus.

Family Ingelarellidae Campbell, 1959
Subfamily Ingelarellinae Campbell, 1959
Genus *Martiniopsis* Waagen, 1883

Type species.—*Martiniopsis inflata* Waagen, 1883.

Martiniopsis sp.
Fig. 6A

Material.—One specimen, external and internal moulds of a ventral valve, NU-B2297.

Remarks.—The single ventral valve specimen from Mt. Tashiroyama can be assigned to the genus *Martiniopsis* Waagen, 1883 by the long, slender subparallel dental adminicula in the ventral valve and in having no impressions of costae on the valve. The Kitakami species closely resembles *Martiniopsis inflata* Waagen (1883, p. 525, pl. 41, figs. 7, 8, text-fig. 9), from the Chhidru Formation of the Salt Range, in the medium size (length more than 17 mm, width about 35 mm) and transverse outline. *Martiniopsis cathaysiensis* Grabau (1936, p. 242, pl. 21, figs. 7, 8; pl. 24, fig. 9), from the Maping Limestone of Guangxi, central-southern China and Guizhou, southwestern China, is also transversely wider in outline but much smaller in size. An accurate comparison is difficult for this poorly preserved specimen.

Order Spiriferinida Ivanova, 1972
Suborder Spiriferinidina Ivanova, 1972
Superfamily Pennospiriferinoidea Dagys, 1972
Family Spiriferellinidae Ivanova, 1972
Genus *Crenispirifer* Stehli, 1954

Type species.—*Spiriferina angulata* King, 1931.

Crenispirifer sagus Cooper and Grant, 1976b
Fig. 6B

Crenispirifer sagus Cooper and Grant, 1976b, p. 2715, pl. 718, figs. 1–15.

Material.—One specimen, external and internal moulds of a dorsal valve, NU-B2298.

Remarks.—This specimen is referred to *Crenispirifer sagus* Cooper and Grant (1976b, p. 2715, pl. 718, figs. 1–15), from the Bone Spring Formation (lower Leonardian) of Texas, by the medium size (length about 10 mm, width about 16 mm in the single dorsal valve) and in having rather numerous costae (numbering 4 on each lateral slope of the dorsal valve) and external surface of the valve ornamented with numerous very fine pustules. *Crenispirifer nakamurai* Tazawa and Shintani (2014, p. 36, figs. 6.11, 6.12), from the Nakadaira Formation (Sakmarian) of Kamiyasse, South Kitakami Belt, differs from *C. sagus* in having more stout costae on the dorsal valve. *Crenispirifer alpheus* (Huang, 1933, p. 59, pl. 9, figs. 2, 3), from the Lopingian of Guizhou, southwestern China, differs from the present species in being smaller size. The type species, *Crenispirifer angulatus* (King, 1931), redescribed by Cooper and Grant (1976b, p. 2710, pl. 716, figs. 1–70; pl. 717, figs. 23–43; pl. 719, figs. 41–47), from the Bone Spring, Skinner Ranch and Gibolo formations of Texas, differs from *C. sagus* in the larger size and in having larger number of costae on the dorsal valve.

Distribution.—Artinskian–Kungurian: northeastern Japan (Nagaiwa–Sakamotozawa in the South Kitakami Belt) and USA (Texas).

Acknowledgements

We sincerely thank Atsushi Matsuoka (Faculty of Science, Niigata University) and an anonymous reviewer for their critical readings of the manuscript; and Yousuke Ibaraki (Fossa Magna Museum, Itoigawa) for his help in drawing figures.

References

Archbold, N. W., 1999, Additional records of Permian brachiopods from near Rat Buri, Thailand. *Proc. Roy. Soc. Vict.*, **111**, 71–86.

Booker, F. W., 1932, A new species of *Productus* from the lower Bowen Series—Queensland. *Proc. Roy. Soc. Qld.*, **43**, 66–72.

Boucot, A. J., Johnson, J. G. and Staton, R. D., 1964, On some atrypoid, retzioid, and athyridoid Brachiopoda. *Jour. Paleont.*, **38**, 805–822.

von Buch, L., 1834, Über Terebrateln, mit einem Versuch sie zu klassifizieren und zu beschreiben. *Phys. Abh. König. Akad. Wis., 1833*, 1–124.

Brunton, C. H. C., Lazarev, S. S., Grant, R. E. and Jin, Y.-G., 2000, Productidina. *In* Kaesler, R. L., ed., *Treatise on Invertebrate Paleontology, Part H Brachiopoda Revised, Volume 3: Linguliformea, Craniiformea, and Rhynchonelliformea (Part)*. Geol. Soc. Amer., Boulder and Univ. Kansas, Lawrence, 424–609.

Campbell, K. S. W., 1959, The *Martiniopsis*-like spiriferids of the Queensland Permian. *Palaeontology*, **1**, 333–350.

Carlson, S. J. and Grant, R. E., 2002, Stenoscismatoidea. *In* Kaesler, R. L., ed., *Treatise on Invertebrate Paleontology, Part H Brachiopoda Revised, Volume 4: Rhynchonelliformea (Part)*. Geol. Soc. Amer., Boulder and Univ. Kansas, Lawrence, 1218–1230.

Carter, J. L. and Gourvennec, R., 2006, Martinioidea. *In* Kaesler, R. L, ed., *Treatise on Invertebrate Paleontology, Part H Brachiopoda Revised, Volume 5: Rhynchonelliformea (Part)*. Geol. Soc. Amer., Boulder and Univ. Kansas, Lawrence, 1747–1768.

Chao, Y.-T., 1929, Carboniferous and Permian spiriferids of China. *Palaeont. Sin., Ser. B*, **11**, 1–133.

Chen, Z.-Q., 2004, Lower Permian reef-dwelling brachiopod faunas from the Tarim Basin, Northwest China: biostratigraphy, palaeoecology and biogeography. *Palaeontogr., Abt. A*, **272**, 1–96.

Conrad, T. A., 1839, Descriptions of new species of organic remains. Second annual report on the Palaeontological Department of the Society. *New York State Geol. Surv., Sec. Ann. Rep.*, 57–66.

Cooper, G. A. and Grant, R. E., 1974, Permian brachiopods of West Texas, 2. *Smithson. Contr. Paleobiol.*, no. 15, 233–793.

Cooper, G. A. and Grant, R. E., 1975, Permian brachiopods of West Texas, 3. *Smithson. Contr. Paleobiol.*, no. 19, 795–1921.

Cooper, G. A. and Grant, R. E., 1976a, Permian brachiopods of West Texas, 4. *Smithson. Contr. Paleobiol.*, no. 21, 1923–2607.

Cooper, G. A. and Grant, R. E., 1976b, Permian brachiopods of West Texas, 5. *Smithson. Contr. Paleobiol.*, no. 24, 2609–3159.

Dagys, A. S., 1972, Morphology and systematics of Mesozoic retzioid brachiopods. *Tr. Inst. Geol. Geofiz., Akad. Nauk SSSR, Siber. Otd.*, **112**, 94–105 (in Russian).

Girty, G. H., 1929, New Carboniferous invertebrates 2. *Jour. Wash. Acad. Sci.*, **19**, 406–415.

Grabau, A. W., 1936, Early Permian fossils of China, Part 2. Fauna of the Maping Limestone of Kwangsi and Kweichow. *Palaeont. Sin., Ser. B*, **8**, 1–441.

Grant, R. E., 1976, Permian brachiopods from southern Thailand. *Jour. Paleont.*, **50** (supp., no. 3), 1–269.

Grunt, T. A., 1986, Classification of brachiopods of the order Athyridida. *Tr. Paleont. Inst., Akad. Nauk SSSR*, **215**, 1–200 (in Russian).

Hall, J. and Clarke, J. M., 1893, *An Introduction to the Study of the Genera of Palaeozoic Brachiopoda, Palaeontology of New York, Volume 8, Part 2*. Charles van Benthuysen and Sons, Albany. 317 p.

Hayasaka, I. and Minato, M., 1956. Some brachiopods from the lower Kanokura Series of the Kitakami Mountains, Japan. *Trans. Proc. Palaeont. Soc. Japan, N. S.*, no. 21, 141–147.

He, X.-L. and Zhu, M.-L., 1979, A new form of brachiopods and its systematical classification. *Jour. Chin. Inst. Min. Tech.*, no. 4, 131–140 (in Chinese).

Huang, T.-K., 1933, Late Permian Brachiopoda of southwestern China, Part 2. *Palaeont. Sin., Ser. B*, **9**, 1–172.

Ivanova, E. A., 1972, Main features of spiriferid evolution (Brachiopoda). *Paleont. Zhur.*, no. 1972-3, 28–42 (in Russian).

Kanmera, K. and Mikami, T., 1965a, Succession and sedimentary features of the Lower Permian Sakamotozawa Formation. *Mem. Fac. Sci., Kyushu Univ., Ser. D*, **16**, 265–274.

Kanmera, K. and Mikami, T., 1965b, Fusuline zonation of the Lower Permian Sakamotozawa Series. *Mem. Fac. Sci., Kyushu Univ., Ser. D*, **16**, 275–320.

Kawamura, T., Uchino, T., Kawamura, M., Yoshida, K., Nakagawa, M. and Nagata, H., 2013, *Geology of Hayachine San District; Quadrangle Series, 1:50,000. Geological Survey of Japan, AIST*. Maeda Insatsu, Tsukuba. 101 p. (in Japanese).

King, R. E., 1931, The geology of the Glass Mountains, Texas, Part 2. Faunal summary and correlation of the Permian formations with description of Brachiopoda. *Univ. Texas Bull.*, no. 3042, 1–245.

Kuhn, O., 1949, *Lehrbuch der Paläozoologie*. E. Schweizerbart. Verlagsbuchhandl., Stuttgart, 326 p.

Lee, L. and Gu, F., 1980, Late Carboniferous brachiopods from Yanji of Jilin, NE China. *Acta Palaeont. Sin.*, **19**, 483–492 (in Chinese).

Liang, W.-P., 1990, *Lengwu Formation of Permian and its Brachiopod Fauna in Zhejiang Province*. Geol. Mem., Ser. 2, No. 10, Geol. Publ. House, Beijing, 522 p. (in Chinese).

Marcou, J., 1858, *Geology of North America, with Two Reports on the Prairies of Arkansas and Texas, the Rocky Mountains of New Mexico and the Sierra Nevada of California*. Zürcher und Furrer, Zürich, 144 p.

M'Coy, F., 1844, *A Synopsis of the Characters of the Carboniferous Limestone Fossils of Ireland*. Williams and Norgate, London, 207 p.

Minato, M., Nakamura, K., Choi, D. R. and Kato, M., 1979, Chapter 2k2. The Sakamotozawa Series. *In* Minato, M., Hunahashi, M., Watanabe, J. and Kato, M. eds., *Variscan Geohistory of Northern Japan: The Abean Orogeny*. Tokai Univ. Press, Tokyo, 174–176.

Mou, C.-J. and Liu, C.-L., 1989, A new type of brachiopods—*Guangdongina* and its ecological environment. *Acta Palaeont. Sin.*, **28**, 455–462 (in Chinese).

Muir-Wood, H. M. and Cooper, G. A., 1960, *Morphology, Classification and Life Habits of the Productoidea (Brachiopoda)*. Geol. Soc. Amer. Mem. 81, Geol. Soc. Amer., New York, 447 p.

Oehlert, D. P., 1887, Appendice sur les brachiopodes. *In* Fischer, P., *Manuel de Conchyliologie et de Paléontologie conchyliologique ou Histoire naturelle des Mollusques vivants et fossils, Vol. 4, Part 11*, Lib. F. Savy, Paris, 1189–1334.

Onuki, Y., 1937, On the Palaeozoic formation near Sakamotozawa, Kitakami Mountainland. *Jour. Geol. Soc. Japan*, **44**, 168–186 (in Japanese).

Onuki, Y., 1969, Geology of the Kitakami Massif, Northeast Japan. *Contr. Inst. Paleont., Tohoku Univ.*, no. 69, 1–239 (in Japanese).

Pavlova, E. E., 1991, Systematical part; Family Spiriferidae. *In* Tatarinov, L. P., Luvsandansan, B., Afanasjeva, G. A., Barsbold, R., Morosova, I. P., Novitskaja, L. I., Rasnitsyn, A. P., Reschetov, V. Yu., Posanov, A. Yu., Sysoev, V. A. and Trofimov, B. A., eds., *Permian Invertebrates of Southern Mongolia. The Joint Soviet–Mongolian Paleontological Expedition, Transactions, Volume 40*, Nauka, Moskva, 124–138 (in Russian).

Sarytcheva, T. G., ed., 1977, Late Palaeozoic productids of Siberia and Arctic Russia. *Tr. Paleont. Inst., Akad. Nauk SSSR*, **161**, 1–220 (in Russian).

Sarytcheva, T. G. and Sokolskaya, A. N., 1959, On the classification of pseudopunctate brachiopods. *Doklady, Akad. Nauk SSSR*, **125**, 181–184 (in Russian).

Shen, S.-Z. and Tazawa, J., 2014, *Pararigbyella* and *Dicystoconcha* (Lyttoniidina, Brachiopoda) from the middle Permian (Wordian) of Japan. *Paleont. Res.*, **18**, 245–249.

Shi, G. R. and Tazawa, J., 2001, *Rhnchopora* and *Blasispirifer* (Brachiopoda) from the middle Permian of the Hida Gaien Belt, central Japan, and their paleobiogeographical significance. *Jour. Geol. Soc. Japan*, **107**, 755–761.

Shintani, T., 2011, Orthotetoids from the Lower Permian (Sakmarian) of the Nagaiwa–Sakamotozawa area, South Kitakami Belt, northeast Japan. *Sci. Rep., Niigata Univ. (Geol.)*, no. 26, 73–90.

Sone, M., Metcalfe, I. and Leman, M. J., 2003, Palaeobiogeographic implications of Middle Permian brachiopods from Johore (Peninsular Malaysia). *Geol. Mag.*, **140**, 523–538.

Sowerby, J., 1818–1821, *The Mineral Conchology of Great Britain, Volume 3*. W. Ardling, London, 184 p.

Stehli, F. G., 1954, Lower Leonardian Brachiopoda of the Sierra Diablo. *Bull. Amer. Mus. Nat. Hist.*, **105**, 262–358.

Stehli, F. G., 1956, Notes on oldhaminid brachiopods. *Jour. Paleont.*, **30**, 305–313.

Stepanov, D. L., 1946, Upper Paleozoic brachiopods from Aldan Basin (Yakutsk, USSR). *Vest. Leningrad. Gosudarstv. Univ.*, no. 93, 196–222 (in Russian).

Tazawa, J., 2001, Middle Permian brachiopods from the Moribu area, Hida Gaien Belt, central Japan. *Paleont. Res.*, **5**, 283–310.

Tazawa, J., 2008a, Permian brachiopods from the Mizukoshi Formation, central Kyushu, SW Japan: Systematics, palaeobiogeography and tectonic implications. *Paleont. Res.*, **12**, 37–61.

Tazawa, J., 2008b, Brachiopods from the Upper Permian Takakurayama Formation, Abukuma Mountains, northeast Japan. *Sci. Rep., Niigata Univ. (Geol.)*, no. 23, 13–53.

Tazawa, J., 2015, Systematics and palaeobiogeography of Permian brachiopods from Pliocene conglomerate of Hitachi, central Japan. *Sci. Rep., Niigata Univ. (Geol.)*, no. 30, 57–88.

Tazawa, J., 2018, Palaeobiogeographical studies on the Palaeozoic brachiopods of Japan, and their tectonic significance: A review. *Jour. Geol. Soc. Japan*, **124**, 655–673 (in Japanese).

Tazawa, J. and Araki, H., 2018, Middle Permian (Wordian) brachiopod fauna from Matsukawa, South Kitakami Belt, Japan, Part 2. *Sci, Rep., Niigata Univ, (Geol.)*, no. 33, 9–24.

Tazawa, J. and Ibaraki, Y., 2001, Middle Permian brachiopods from Setamai, the type locality of the Kanokura Formation, southern Kitakami Mountains, northeast Japan. *Sci. Rep., Niigata Univ. (Geol.)*, no. 16, 1–33.

Tazawa, J., Kaneko, N., Suzuki, C. and Hasagawa, S., 2015, Late Permian (Wuchiapingian) brachiopod fauna from the lower Takakurayama Formation, Abukuma Mountains, northeastern Japan. *Paleont. Res.*, **19**, 33–51.

Tazawa, J., Kikuchi, Y., Nikaido, A., Adachi, S. and Okumura, Y., 2014, Permian brachiopods from boulders in the Pliocence basal conglomerate of Hitachi, central Japan. *Jour. Geol. Soc. Japan*, **120**, 377–391 (in Japanese).

Tazawa, J. and Nakamura, K., 2015, Early Permian (Kungurian) brachiopods from Nakadaira, South Kitakami Belt, northeastern Japan. *Paleont. Res.*, **19**, 156–177.

Tazawa, J. and Shintani, T., 2010, A lower Permian mixed Boreal–Tethyan brachiopod fauna from the Nagaiwa–Sakamotozawa area, South Kitakami Belt, NE Japan. *Sci. Rep., Niigata Univ. (Geol.)*, no. 25, 51–62.

Tazawa, J. and Shintani, T., 2014, Early Permian (Sakmarian) brachiopods from Kamiyasse, South Kitakami Belt, northeast Japan. *Sci. Rep., Niigata Univ. (Geol.)*, no. 29, 13–41.

Tazawa, J. and Shintani, T., 2015, Early Permian (Sakmarian) brachiopods from the Nagaiwa–Sakamotozawa area, South Kitakami Belt, northeastern Japan, Part 3: Productidina. *Sci. Rep., Niigata Univ. (Geol.)*, no. 30, 39–55.

Termier, G., Termier, H., de Lapparent, A. F. and Marin, P., 1974, Monographie du Permo–Carbonifère de Wardak (Afghanistan central). *Doc. Lab. Géol. Fac. Sci. Lyon, Hors Ser.*, **2**, 1–167.

Tscernyschew, Th., 1902, Die obercarbonischen Brachiopoden des Ural und des Timan. *Tr. Geol. Kom.*, **16**, 1–749 (in Russian).

Ueno, K., Shintani, T. and Tazawa, J., 2009, Fusuline foraminifera from the upper part of the Sakamotozawa Formation, South Kitakami Belt, Northeast Japan. *Sci. Rep., Niigata Univ. (Geol.)*, no. 24, 27–61.

Ueno, K., Shintani, T. and Tazawa, J., 2011, A fusuline fauna from the basal part of the Sakamotozawa

Formation in the Kamiyasse area, South Kitakami Belt, Northeast Japan. *Sci. Rep., Niigata Univ. (Geol.)*, no. 26, 23–41.

Ueno, K., Tazawa, J. and Shintani, T., 2007, Fusuline foraminifera from the basal part of the Sakamotozawa Formation, South Kitakami Belt, Northeast Japan. *Sci. Rep., Niigata Univ. (Geol.)*, no. 22, 15–33.

Waagen, W., 1883–1884, Salt Range fossils, Vol. 1, Part 4. *Productus* Limestone fossils, Brachiopoda. *Palaeont. Ind., Ser. 13*, fasc. 2, 391–546 (1883), fasc. 3, 547–610 (1884) and fasc. 4, 611–728 (1884).

Wang, G., Liu, Q., Jin, Y., Hu, S., Liang, W. and Liao, Z., 1982, Phylum Brachiopoda. *In* Nanjing Institute of Geology and Mineral Resources, *ed., Palaeontological Atlas of East China, Part 2. Volume of Late Palaeozoic*. Geol. Publ. House, Beijing, 186–256 (in Chinese).

Wang, H.-Y. and Jin, Y.-G., 1991, On permianellids (Brachiopoda). *Acta Palaeont. Sin.*, **30**, 481–501 (in Chinese).

Waterhouse, J. B., 1968, Classification and descriptions of Permian Spiriferida (Brachiopoda) from New Zealand. *Palaeontogr., Abt. A*, **129**, 1–94.

Waterhouse, J. B., 1975, New Permian and Triassic brachiopod taxa. *Univ. Qd. Pap., Dept. Geol.*, **7**, 1–23.

Waterhouse, J. B. and Piyasin, S., 1970, Mid-Permian brachiopods from Khao Phrik, Thailand. *Palaeontographica, Abt. A*, **135**, 83–197.

Williams, A., 1953, The classification of the strophomenoid brachiopods. *Wash. Acad. Sci. Jour.*, **43,** 1–13.

Williams, A., Harper, D. A. and Grant, R. E., 2000: Lyttoniidina. *In* Kaesler, R., *ed., Treatise on Invertebrate Paleontology, Part H Brachiopoda Revised, Volume 3: Linguliformea, Craniiformea, and Rhynchonelliformea (Part)*, Geol. Soc. Amer., Boulder and Univ. Kansas, Lawrence, 619–642.

Yanagida, J., 1970, Permian brachiopods from Khao Phrik, near Rat Buri, Thailand. *Geol. Palaeont. SE Asia*, **8**, 69–96.

Yamada, Y., 1959, On the unconformity of the post-Nagaiwa—pre-Sakamotozawa epoch in the Hikoroichi district. *Jour. Geol. Soc. Japan*, **65**, 713–724 (in Japanese).

Yanagida, J. and Nakornsri, N., 1999, Permian brachiopods from the Khao Hin Kling area near Phetchabun, north-central Thailand. *Bull. Kitakyushu Mus. Nat. Hist.*, no. 18, 105–136.

Yang, D., 1984, Systematic description of palaeontology; Brachiopoda. *In* Yichang Institute of Geology and Mineral Resources, *ed., Biostratigraphy of the Yangtze Gorge Area, (3) Late Palaeozoic Era*, Geol. Publ. House, Beijing. 203–239, 330–333 and 387–396 (in Chinese).

A new inlet system for microscale carbon and oxygen stable isotope analysis using dual inlet isotope ratio mass spectrometer at Niigata University, Japan

Madhusoodhan SATISH-KUMAR*, Sasidharan KIRAN** and Miyako ABE**

Abstract

A new Thermo Scientific™ MAT-253 isotope ratio mass spectrometer was installed at Department of Geology, Niigata University, Japan under the MEXT Grant-in-Aid for Scientific Research on Innovative Areas. The mass spectrometer was set up for carbon and oxygen isotope measurement of small volume CO_2 samples. A new inlet vacuum line was constructed for transferring standard gas, to inlet externally prepared CO_2 gas samples and transfer CO_2 gas prepared in the online carbonate reaction system. The line is evacuated using a turbo molecular pump and pneumatically activated valves controlled by an electrical control board. The vacuum line also includes a reference CO_2 gas (Working Standard) reservoir and a laboratory standard CO_2 gas (Machine Standard) reservoir for routine analyses, as well as SF_6 reference gas reservoirs. The preparation line can hold high vacuum conditions without appreciable leaks for several hours, required for the completion of a single session of sample measurements. Long-term laboratory standard measurement results are reported here, which shows an average of $\delta^{13}C_{(V\text{-}PDB)}$ value of –29.796 ± 0.041‰ and $\delta^{18}O_{(V\text{-}SMOW)}$ value of 3.971 ± 0.062‰ (n = 44; 1 σ). During a period of one year of analysis, a drift of 0.04‰ for both carbon and oxygen is observed for the reference CO_2 gas. NIST standards (NBS-20 limestone and NBS-21 graphite) and a laboratory diamond standard were analyzed to characterize the minimum volume of sample required to obtain carbon and oxygen isotopic composition with accuracy and precision <0.1‰. We also report here the routine analytical procedure for carbonate samples (calcite/aragonite and dolomite/siderite/magnesite) and elemental carbon (graphite and diamond).

* Department of Geology, Faculty of Science, Niigata University, 2-8050 Ikarashi, Nishi-ku, Niigata 950-2181, JAPAN

Corresponding author: M. Satish-Kumar, satish@geo.sc.niigata-u.ac.jp

** Graduate School of Science and Technology, Niigata University, 2-8050 Ikarashi, Nishi-ku, Niigata 950-2181, JAPAN

(Manuscript received 1 March, 2021; accepted 20 March, 2021)

Key words: carbon and oxygen isotopes, MAT-253 inlet system, NIST standard measurements.

Introduction

A new Thermo Scientific™ MAT-253 isotope ratio mass spectrometer (IRMS) was installed at Department of Geology, Niigata University, Japan under the MEXT Grant-in-Aid for Scientific Research on Innovative Areas. Here we report the analytical set up for carbon and oxygen isotope measurements for small volume samples. Conventionally, stable isotope measurements of carbon and oxygen isotopes are carried out using CO_2 gas in a dual inlet gas source mass spectrometer (Nier et al., 1947; Hoefs, 1997). In order to measure a sample gas using a dual inlet gas source mass spectrometer, it is essential to have a reference CO_2 gas reservoir. Carbon and oxygen isotopes are measured by simultaneously acquiring the CO_2^+ ions in the Faraday cup at m/z 44 ($^{12}C^{16}O^{16}O$), 45 ($^{13}C^{16}O^{16}O$) and 46 ($^{12}C^{18}O^{16}O$).

Carbon isotopes are conventionally expressed as $\delta^{13}C$ values (in ‰) to the Pee Dee Belemnite (PDB) scale (Craig, 1957), which was later on revised to the V-PDB scale (Coplen, 1988, 1994, 1996). The primary standards that are available include NBS-19 and NBS-20, and both have been assigned carbon isotopic values on the V-PDB scale. Oxygen isotopes, commonly expressed as $\delta^{18}O$ values (in ‰) to the standard mean ocean water (SMOW) scale (Craig, 1957), which was later on revised to the international V-SMOW scale (Coplen, 1988). The V-SMOW scale is fixed by the standards V-SMOW and standard light Antarctic precipitation (SLAP), having assigned isotopic values. Conversion equations for oxygen isotope values for carbonate samples, from one international scale to the other, V-PDB to V-SMOW and vice versa are given below (after Coplen, 1988)

$$\delta^{18}O_{V\text{-}PDB} = 0.97002\ \delta^{18}O_{V\text{-}SMOW} - 29.98$$

$$\delta^{18}O_{V\text{-}SMOW} = 1.03091\ \delta^{18}O_{V\text{-}PDB} + 30.91$$

A new inlet vacuum line for transferring reference gas and sample gas to the built-in reservoirs in the mass spectrometer, to inlet offline CO_2 gas samples and CO_2 gas from online carbonate reaction system were built. In the following sections, we describe the basic set up of IRMS, the components of the inlet vacuum line and results of international standards in detail. A companion paper will describe the instrumental set up for multiple sulfur isotope measurements and sample preparation for SF_6 gas from rock samples with sulfide minerals.

Basic set up of IRMS

The dual inlet gas source IRMS at Niigata University (Fig. 1A) is designed to measure carbon (as CO_2 or CO gas samples), oxygen (as O_2, CO_2 or CO), sulfur (as SF_6), nitrogen (as N_2)

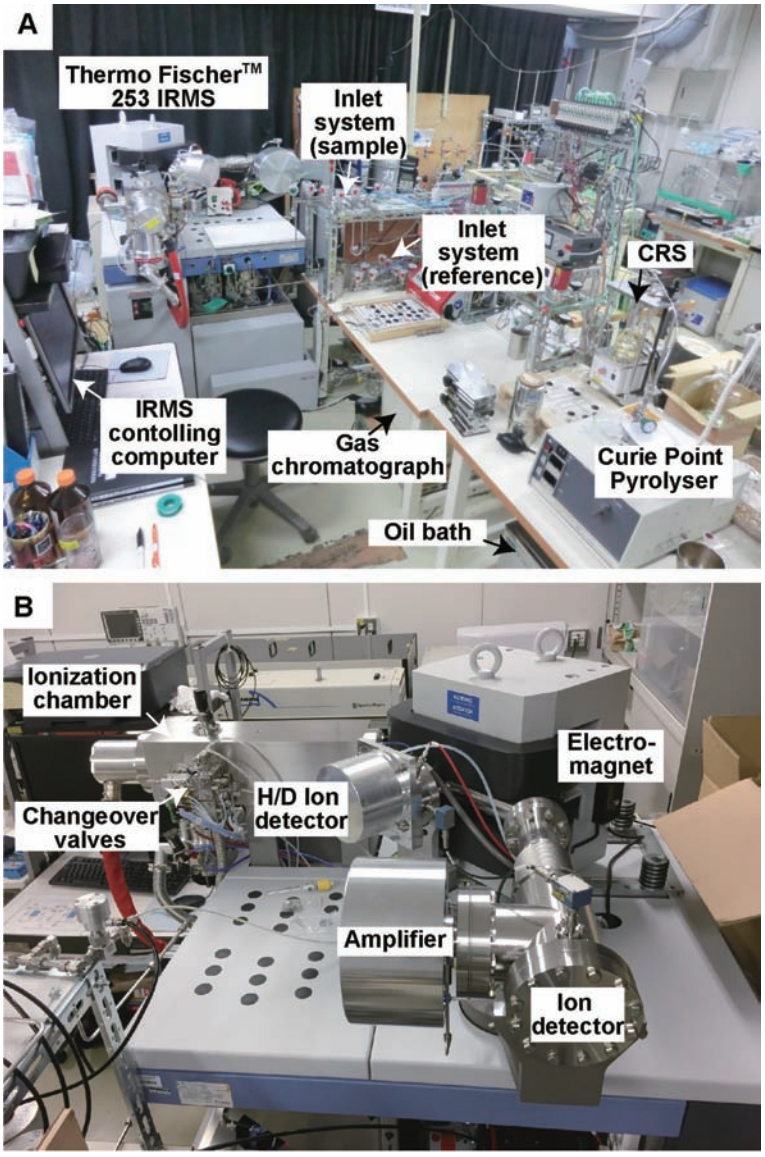

Fig. 1. A) Generalized view of the Thermo Scientific™ MAT-253 isotope ratio mass spectrometer and associated gas preparation vacuum lines. B) Enlarged view of ionization chamber, changeover valves, the detection chamber and amplifying unit.

and hydrogen (as H_2) isotopes. The IRMS has a customized collector assembly of 8 Faraday cups, in addition to the H/D collector with 2 Faraday cups (Fig. 1B). The Faraday cups are aligned for the simultaneous measurement of multiple sulfur isotopes of ^{32}S, ^{33}S, ^{34}S and ^{36}S. The alignment of Faraday cups and their respective resistors for amplifiers are shown in Fig. 2. Faraday cups 1, 2 and 4 are used for CO_2 measurements corresponding to resistors of

Slit Width (mm)			3.5	1.5	1.5	1.5	3.5	1.5	1.5	1.5
		Cup No.	1	2	3	4	5	6	7	8
		Ampl. Channel	1	2	3	4	5	6	7	8
Gases/ Masses	44,45,46	**CO2**	44	45		46				
	28,29,30	**N2/CO**	28		29		30			
	32,33,34	**O2**	32		33		34			
	127,128,129,131	**SF6**					127	128	129	131
Resistors (Ohm)		**CO2**	3E+10	3E+8		1E+11				
		N2/CO	3E+8		3E+10		1E+11			
		O2	3E+8		3E+11		1E+11			
		SF6					3E+8	3E+10	1E+10	1E+12

Fig. 2. Schematic sketch showing the alignment of Faraday cups and their respective resistors for amplifier in the mass spectrometer.

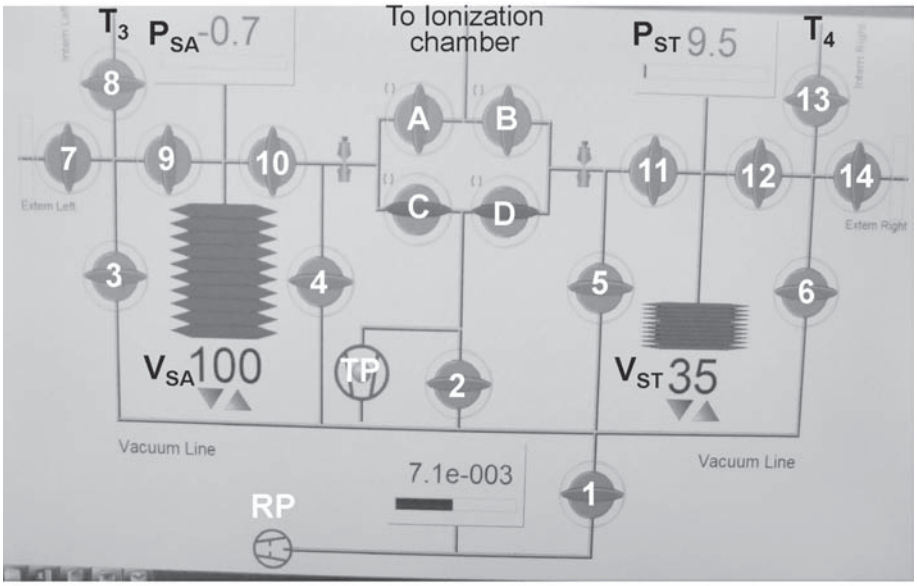

Fig. 3. Schematic layout of the built-in inlet system of the IRMS. The line is evacuated using a turbomolecular pump (TP) or a rotary pump (RP). Sample and reference gas reservoirs (V_{SA} and V_{ST}) are directly connected to two pressure gauges. There are 14 pneumatic computer-controlled valves (Nos. 1 to 14) and a changeover valve (A-D), which switches between sample side and reference side flow of gas to the ionization chamber or to the ion pump.

3×10^{10}, 3×10^{8} and 1×10^{11} ohms, respectively. The IRMS was set up for routine measurement of carbon and oxygen isotopes using carbon dioxide as a gas medium.

The built-in inlet system of the IRMS comprises of two gas reservoirs and a series of pneumatic valves as shown in Fig. 3. The line is connected to the external inlet system through 1/4" connectors; the sample side is being connected through the valve No. 7 and

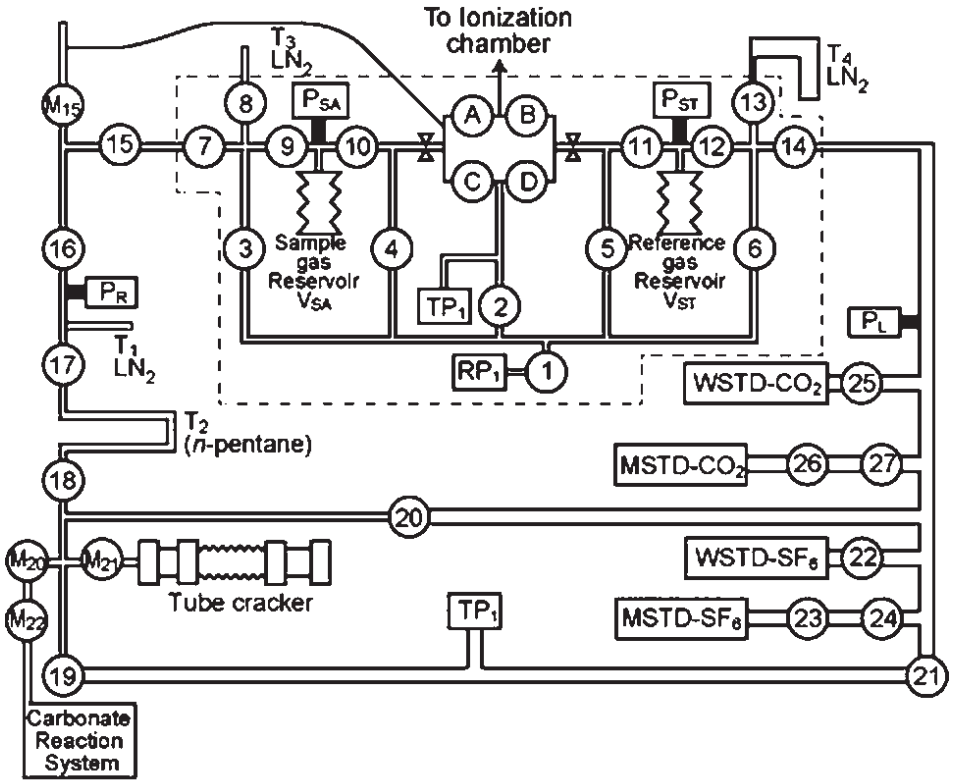

Fig. 4. Schematic layout of the vacuum line reference and laboratory standard gas reservoirs connected to the IRMS. The section demarcated using a dashed line is the built-in-inlet system of the IRMS. Thickness of tubes corresponds to 3/8" or 1/4" diameter tubes and connectors. Abbreviations are; CRS: Carbonate reaction system; M_1, M_2: Manual valves; MASS SA: Capillary connection of sample gas to ionization chamber; MASS ST: Capillary connection of standard gas to ionization chamber; MSTD-CO_2: Machine standard CO_2 gas reservoir; WSTD-CO_2: Working standard CO_2 gas reservoir; MSTD-SF_6: Machine standard SF_6 gas reservoir; WSTD-SF_6: Working standard SF_6 gas reservoir; P_1-P_2: Pirani gauge sensors; T_1, T_3-T_4: Liquid nitrogen traps; T_2: Pentane slush; TP: Turbo pump; Numerals 14 to 28 represent pneumatic bellows valves.

standard side through valve No. 14 (Fig. 3). The volume of the sample and standard reservoirs (V_{SA} and V_{ST}) can be adjusted from c. 3 cc to c. 40 cc and both the reservoirs are directly connected to pressure gauges (P_{SA} and P_{ST}) for monitoring the pressure of the gas inside the reservoirs (Fig. 3). The valves were numbered from 1 to 14 and the changeover valves as A, B, C and D (Fig. 3). The vacuum line can be evacuated either by a rotary pump (RP) or a turbo molecular pump (TP) (Fig. 3).

Gas inlet system

The structure of the newly built inlet vacuum line follows the design described in detail in Wada et al. (1982, 1984a, b, 2008) and is schematically illustrated in Fig. 4. The vacuum

Fig. 5. A broad view of the inlet system for CO_2 and SF_6 standard gas and sample gas for carbon, oxygen and sulfur isotope analysis.

line for reference and standard gases was constructed using a combination of 3/8" and 1/4" stainless steel pipes and connectors (Figs. 5, 6), in order to minimize the dead volume inside the line and for quick transfer of gas to reservoirs. The pipes are connected using Swagelok® joints and Cajon® pneumatic bellows valves (Fig. 6A). The line is evacuated using a turbo molecular pump (PFEIFFER® HiCUBE80 Classic). There are two pressure gauges (P_L and P_R; Pirani gauges, WAKAIDA SCIENCE CORPORATION, PG-2B02), P_L is located at the standard segment in the line and P_R is located at the sample segment (Fig. 4). Altogether, the vacuum line is composed of 14 Cajon® pneumatic bellows valves (Fig. 6B) operated by electromagnetic switches (Fig. 6C), which are controlled by electrical switches in a control board (Fig. 7). In addition, there are 4 manual valves. Manual valve M_{15} is connected to the microvolume gas inlet to the IRMS through the capillary tube (Fig. 4). Manual valves M_{20} and M_{22} connects the carbonate reaction system to the inlet line and the manual valve M_{21} is connected to a flexible tube cracker for breaking 6 mm diameter glass tubes containing CO_2 gas samples prepared offline.

There are 3 cold traps (T_1-T_3) in the CO_2 gas inlet line (Fig. 4). These cold traps are used for cleaning a mixed sample gas containing CO_2 and impurity gases, and separate

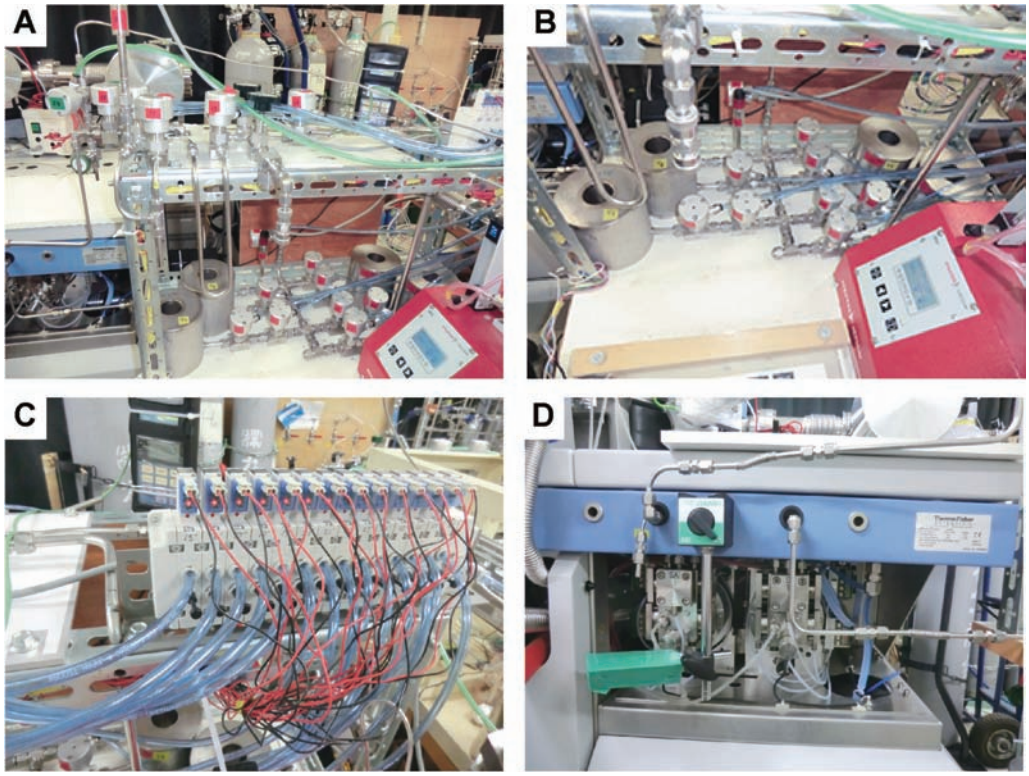

Fig. 6. Photographs showing important segments of the inlet system. A) A general view of the vacuum line. B) Working standard (WSTD) and machine standard (MSTD) gas reservoirs containing CO_2 gas. C) Electromagnetic valves used for opening and closing pneumatic valves in the vacuum line. D) View of the built-in vacuum line and T_3 trap for collecting sample gas.

condensable and non-condensable gases cryogenically. T_1 is 5 cm long stainless-steel tube with a welded cap and T_2 is a U-shaped 3/8" stainless pipe cold trap, (Fig. 6A). These two cold traps are designed to cryogenically separate CO_2, H_2O and other non-condensable gases, using liquid N_2 (–196 °C) and *n*-pentane slush (c. –125 °C), respectively. The n-pentane slush is maintained at a temperature around –125 to –130 °C (Wada et al., 1984a) by constantly cooling it using liquid N_2 and monitored using a thermometer (Fig. 4).

The gas inlet system is connected to the inlet reservoirs and vacuum system of the IRMS by 1/4" stainless steel pipe and flexible tubes. A small volume trap T_3 was set up in the IRMS inlet line using a 3 cm long 1/4" stainless steel tube with a welded cap (Fig. 6D) and filled with stainless steel balls. This cold trap is connected to the inlet line with a 3 mm diameter stainless steel pipe in order to reduce the inner dead volume. A similar assembly system is used in the microvolume trap (MV trap) as well (Fig. 4). The sample gas is transported from T_2 to T_3 cryogenically using liquid nitrogen and then expanded to the sample gas reservoir (V_{SA}) in the IRMS, which is then flowed to the ionization chamber through a capillary tube (Fig. 3).

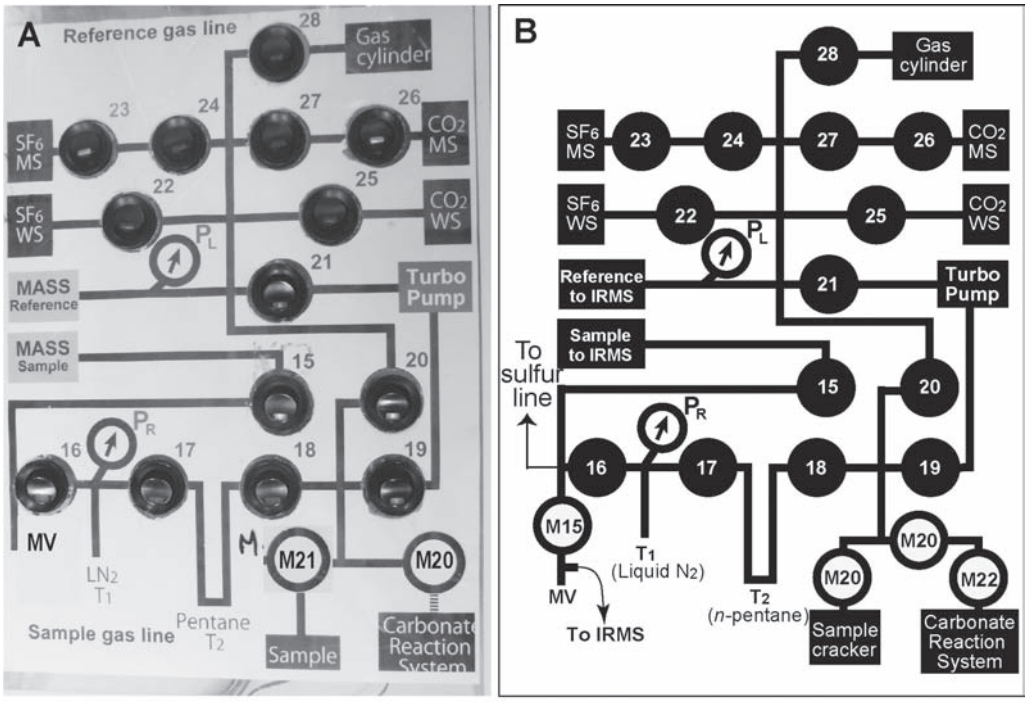

Fig. 7. Electrical switchboard for controlling the pneumatic valves of the inlet system. A) photograph of the control board. B) Sehematie figure showing the mlet system.

Carbonate reaction system

The carbonate reaction system (CRS) was designed based on the specifications given in Wada et al. (1982, 1984a) (Fig. 8A). It consists of a specially designed double chamber reaction vessel made of glass, the inner chamber is connected to the vacuum line and contain phosphoric acid and the outer chamber is used to circulate heated oil from a temperature-controlled oil bath (Fig. 8A). A magnetic stirrer is placed below the reaction vessel and a glass covered magnetic rod is used to stir the sample cups and to make sure that the reaction between carbonate powder and acid is completed (Fig. 8B). The rotating sample holder, made of stainless steel, can hold up to 24 sample cups at a time (Fig. 8B). The temperature-controlled oil bath is used for heating the phosphoric acid to ambient temperature for carbonate digestion (Fig. 8C). The merit of using an oil bath is that the temperatures in the range of 25 to 180 °C can be achieved.

Reaction rate of carbonate samples is dependent on the composition of the carbonate mineral, the surface area of the grains, the reaction temperature and the viscosity of the phosphoric acid. At Niigata University, calcite and aragonite are digested at 60 °C and other carbonates including dolomite and magnesite are digested at 100 °C. Appropriate oxygen isotope fractionation factors from the literature is used to for correcting the data (e. g.

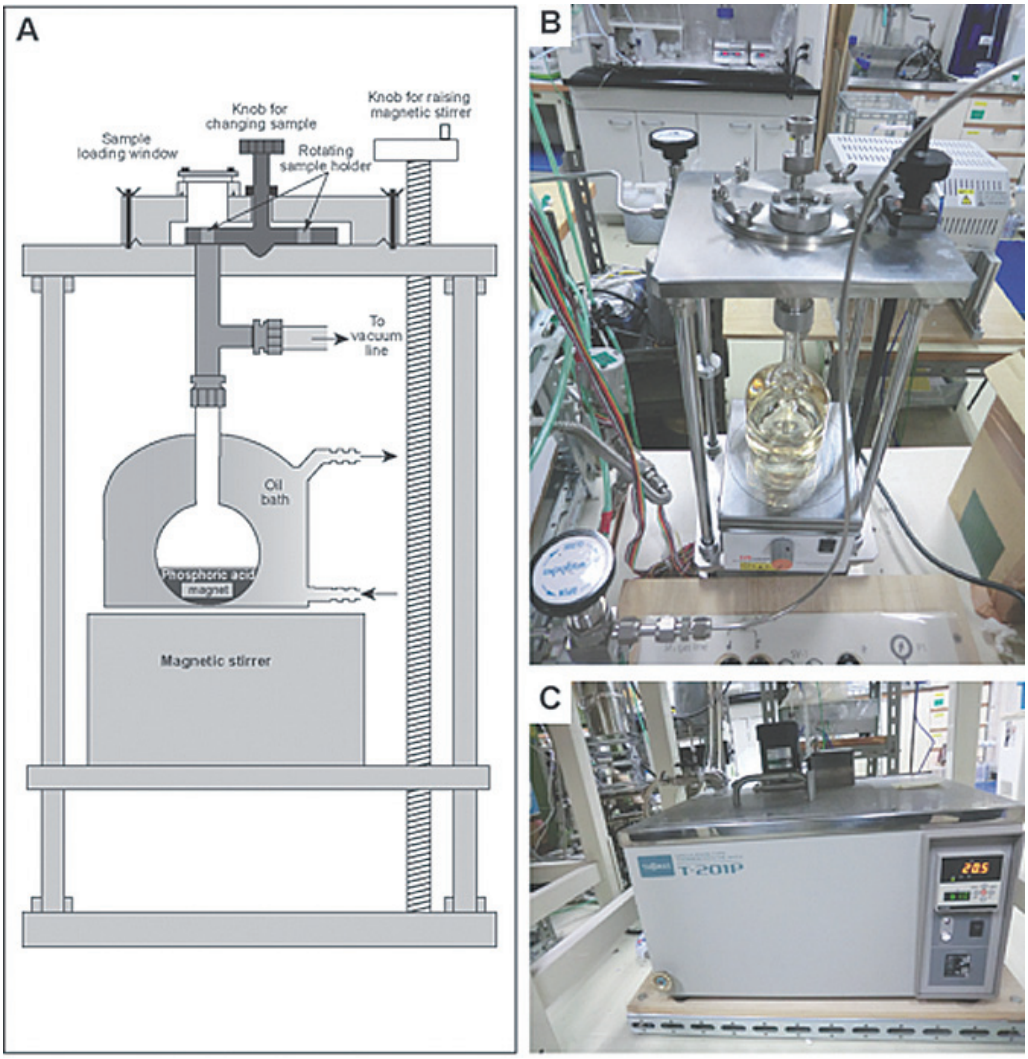

Fig. 8. A) Sketch of the carbonate reaction system (after Wada et al.,1982). B) Photograph of the carbonate reaction system. C) Oil tank with heating unit used for circulating the oil to reaction vessel.

Sharma and Clayton, 1965; Northrop and Clayton, 1966; Rosenbaum and Sheppard, 1986; Cornides and Kusakabe, 1977).

Vacuum condition

Initial vacuum tests of the system were carried out in order to check the high-vacuum condition for intervals of time required for the preparation and analysis of samples during a session of measurement, beginning and ending with laboratory standard (MSTD). A single session usually consists of more than 10 hours of measurements and each sample

measurement can be accomplished within an hour. The system was evacuated overnight to the minimum pressure measured at the pirani gauges (P_L and P_R) and vacuum check was conducted based on the following procedure. Initially, all the valves were kept closed for a specific time (e.g., 12 hours) and then, starting from the valve nearer to the gauge, and valves were opened one by one, while reading the shift in P_L and P_R values. For example, in the case of sample gas inlet segment's vacuum check, P_R is monitored initially with all valves closed. After keeping it for 12 hour the valve Nos. 17, 18, 16 and 15 (Fig. 4) were opened one by one and the shift in P_R is recorded. Similarly, the vacuum condition of the standard gas segment was also tested by monitoring the shifts in P_L values from the minimum value (Fig. 4). The results indicate that all segments in the vacuum line can essentially keep high vacuum condition for more than 12 hours, with limited increase of 0.2 and 0.4 Pa, for P_L and P_R values, respectively. Vacuum condition tests were also performed for the built-in vacuum line of the IRMS, which also indicated that the line could withstand high-vacuum condition for more than 12 hours duration (Fig. 3). These vacuum tests assure that for a single session of measurements there is basically no leaks and thereby confirming that no external contamination of gases to the vacuum system.

Measurement of laboratory standard CO_2 gas

Initial tests were carried out using laboratory machine standard (MSTD) CO_2 gas for determining the precision of carbon and oxygen isotope measurement. The procedure for transferring the reference working standard gas and the measurement of MSTD are given in Appendix 1. The results are shown in Fig. 9. The average values of $\delta^{13}C_{V\text{-}PDB}$ and $\delta^{18}O_{V\text{-}SMOW}$ for MSTD are –29.796 ± 0.041‰ and 3.971 ± 0.062‰ (n = 44; 1 σ), respectively, which shows a very good accuracy and precision (Fig. 9A). The MSTD values were also monitored for long term variations in the reference working standard and the results are presented in Figs. 9B and 9C. During a period of one year of analysis, a drift of 0.04‰ is observed for $\delta^{13}C_{V\text{-}PDB}$ and $\delta^{18}O_{V\text{-}SMOW}$ values for the reference CO_2 gas.

Capillary flow and pressure effect on carbon and oxygen isotopic ratios

The dual inlet system of IRMS utilizes a reference gas (WSTD) and sample gas for the measurement of isotope ratio. These two gases are flowed into the ionization chamber alternatively through capillary tubes connected to the changeover valve A, B, C and D (Fig. 3). The isotope ratio of sample is estimated by repeatedly measuring the reference gas and sample gas. The gas pressure at both sample side and reference side are kept same during the measurement (Wada et al., 2008). The WSTD gas is continuously flowing during the analytical session and therefore it is necessary to monitor the drift in isotope ratio. We have

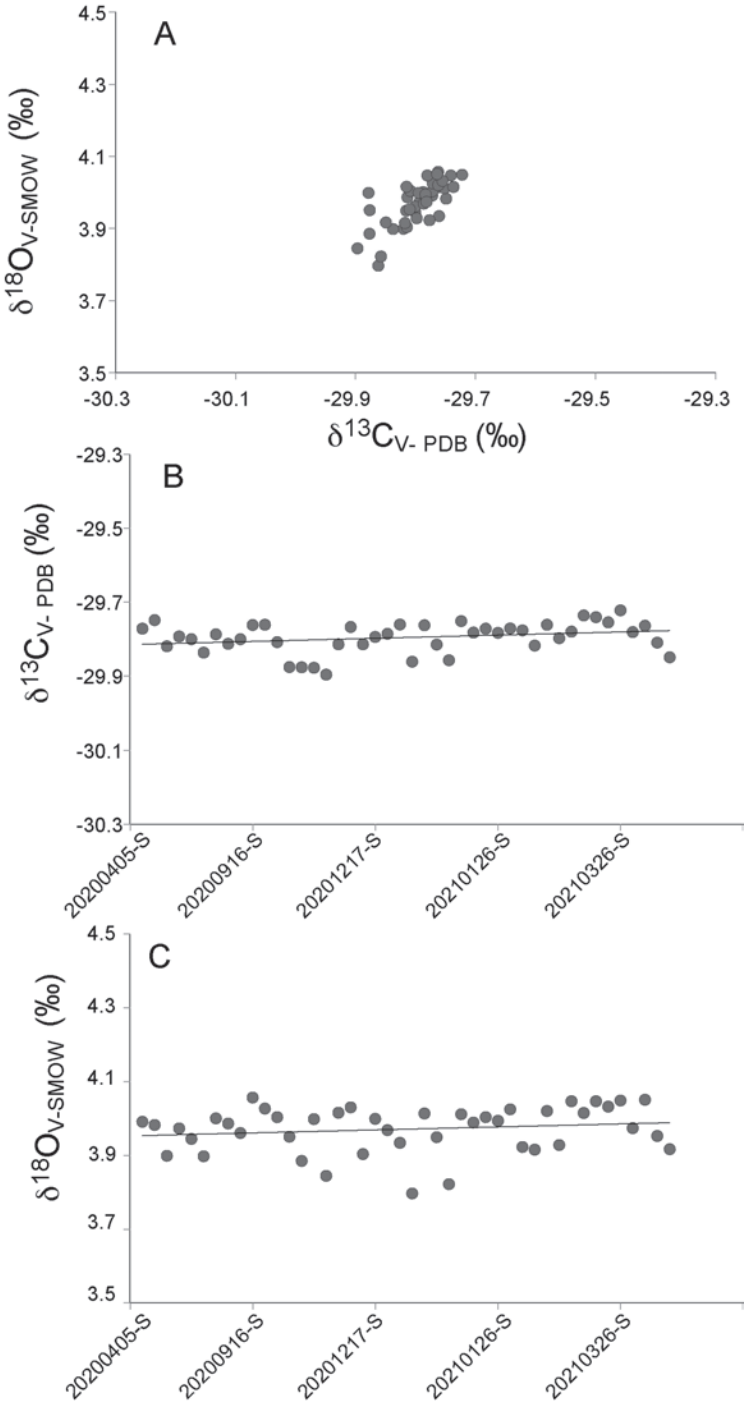

Fig. 9. Long term (one year) drift in carbon and oxygen isotopic composition for CO_2 laboratory standard gas. Forty-four MSTD measurements carried out from April 2020 to March 2021 are presented here. A) $\delta^{13}C_{V\text{-}PDB}$ vs. $\delta^{18}O_{V\text{-}SMOW}$ plot. B) Drift in $\delta^{13}C_{V\text{-}PDB}$ values of MSTD for a period of one year. C) Drift in $\delta^{18}O_{V\text{-}SMOW}$ values of MSTD for a period of one year.

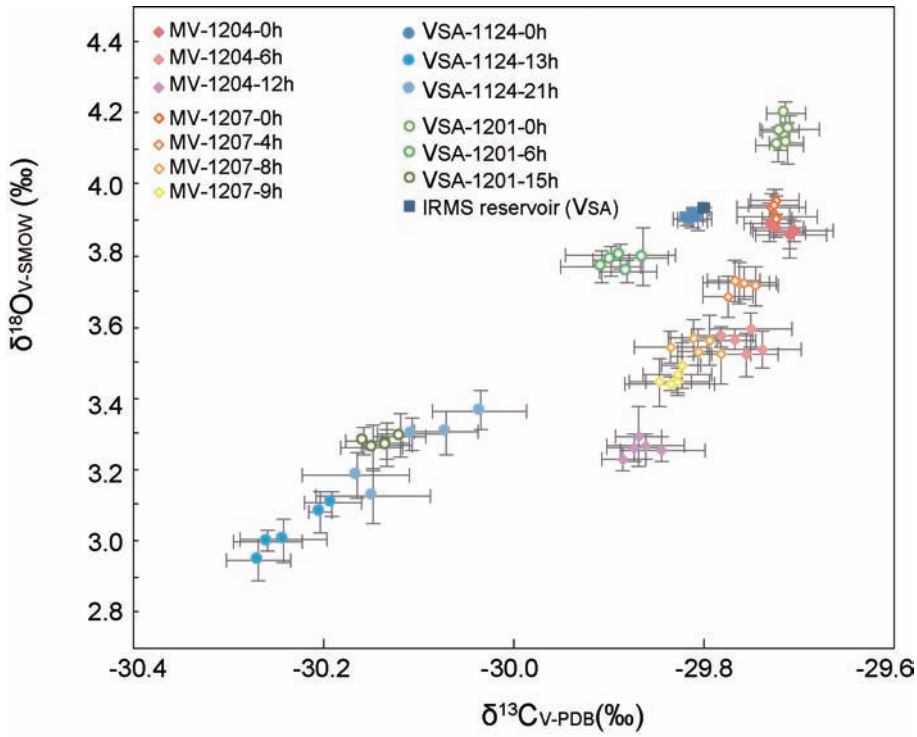

Fig. 10. Fractionation of carbon and oxygen isotopes during capillary flow. MV represents micro volume trap and VSA represents IRMS reservoir.

carried out experiments by continuously measuring the same MSTD gas to monitor the isotope fractionation during capillary flow as well as repeated measurements of MSTD gas. Fig. 10 shows the shift in isotope values of $\delta^{13}C_{V\text{-}PDB}$ and $\delta^{18}O_{V\text{-}SMOW}$ related to elapsed time for reference gas. Each analysis used a new aliquot of MSTD gas.

In the case of MSTD gas flowing continuously from V_{SA} through the capillary, repeated measurements for six hours showed only a drift of –0.17‰ for $\delta^{13}C_{V\text{-}PDB}$, and –0.37‰ for $\delta^{18}O_{V\text{-}SMOW}$ values. On the other hand, in the case of measurements using twice the volume of reference gas, the variation of $\delta^{13}C_{V\text{-}PDB}$ was –0.04‰ and for $\delta^{18}O$ it was –0.32‰. The drift in $\delta^{13}C_{V\text{-}PDB}$ values decreased considerably, although the $\delta^{18}O$ values have some minor shifts even at larger gas flow.

Preparation of phosphoric acid for carbonate digestion

The method for the preparation of phosphoric acid for carbonate acid digestion follows the description given in Bowen (1966) and Coplen et al. (1983) . At first, P_2O_5 is added to 85% H_3PO_4 (orthophosphoric acid) in a weight ratio of 3:7. A small volume of (～10 mg; Coplen et al.,1983) of CrO_3 is added, turning the solution yellow. The solution is heated at ～200 °C for

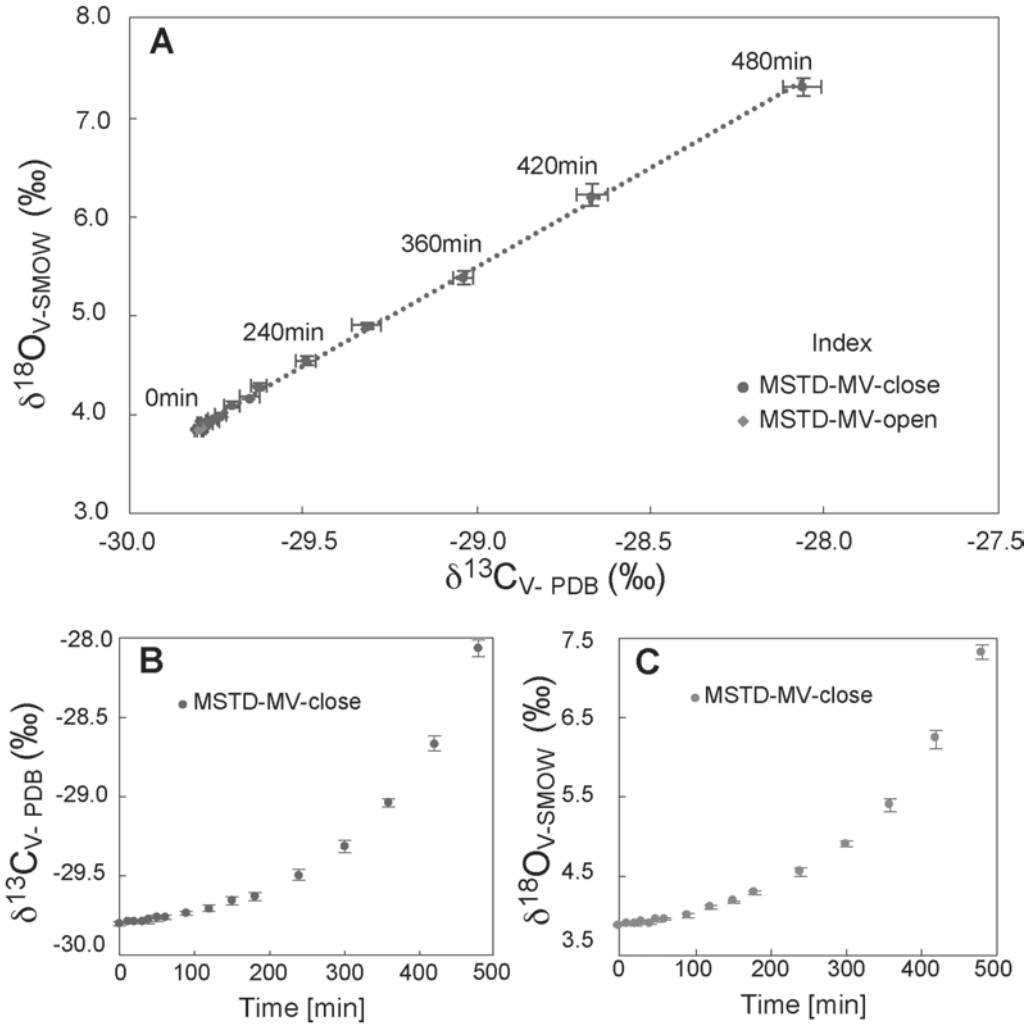

Fig. 11. A) Variation related to analysis time between $\delta^{13}C_{V\text{-}PDB}$ and $\delta^{18}O_{V\text{-}SMOW}$ values in micro-volume trap. B) Variation of carbon isotope in micro-volume trap with time. C) Variation of oxygen isotope in micro-volume trap with time.

7 hours, turning green. A small volume (~3 ml) of H_2O_2 is added and continued to heat at 220 °C for an additional 4.5 hrs. The resulting acid has a chemical formula of $H_4P_2O_7$ (pyrophosphoric acid), and a density of about 1.9 g/cc. This acid is bottled in vacuum to avoid contact with atmosphere, since pyrophosphoric acid is extremely hygroscopic and absorb moisture from the atmosphere if kept open.

Experiments with micro-volume trap

For the micro volume sample gas, we installed the new capillary tube with a micro-

volume trap (MV) directly to the changeover valve (Fig. 4). Using this MV-trap small volume of MSTD gas was measured. The value of MSTD gas filled between valve Nos. 15, 20 and 19 gave $\delta^{13}C_{V\text{-}PDB}$ and $\delta^{18}O_{V\text{-}SMOW}$ values of –29.78 ± 0.01‰ and 3.96 ± 0.01‰, respectively. After this analysis, valve No. 15 was closed and repeatedly analyzed at regular intervals. The value of $\delta^{13}C_{V\text{-}PDB}$ and $\delta^{18}O_{V\text{-}SMOW}$ indicated exponential fractionation related to time (Fig. 11A). The linear trend of δ values between carbon and oxygen indicate a clear mass depended Rayleigh fractionation through the capillary tube as shown by the exponential trend with time for both carbon and oxygen isotopes (Fig. 11B, C). The fractionation of MSTD gas in the micro-volume trap shows a large variation because the fraction of gas remaining in the micro-volume trap and the flowed volume is large enough to cause fractionation.

High precision carbon and oxygen isotope ratios were obtained using this micro-volume trap by adopting the following improvements and optimization of preparation procedure for carbonate and elemental carbon samples following Wada and Itoh (1990). It is possible to analyze ~1 micro-mole CO_2 gas using this micro-volume trap at high precision (<0.1‰ for both $\delta^{13}C_{V\text{-}PDB}$ and $\delta^{18}O_{V\text{-}SMOW}$). The small volume CO_2 sample gas is purified using an *n*-pentane slush, which is maintained at a temperature c.–125 °C, as explained in the previous section. When small carbonate samples are reacted with phosphoric acid, H_2O is also produced in variable amounts depending upon the temperature of reaction. Previous studies have shown that H_2O cannot be completely separated from CO_2 using dry ice or alcohol slush at low partial pressures and further lowering of temperature is essential to reduce the H_2O molecules being trapped in liquid nitrogen trap (Wada et al., 2008).

Measurement of small volume calcite and graphite standard samples

NBS-20 calcite, NBS-21 graphite, laboratory graphite (SP1) standard and a laboratory diamond standard (artificial diamond crystal) were used to test the precision of small volume gas samples measurements. Measurements were carried out using T_3 trap and capillary flow using the built-in-reservoir V_{SA}. The average of $\delta^{13}C_{V\text{-}PDB}$ and $\delta^{18}O_{V\text{-}SMOW}$ values for NBS-20 calcite are 1.03 ± 0.09‰, and 26.22 ± 0.29‰ (1σ; n = 5), respectively for samples weighing from 1.97 mg to 3 mg, which shows very good accuracy and precision (Fig. 12A, B). Samples with lower volume showed systematic lowering of both $\delta^{13}C_{V\text{-}PDB}$ and $\delta^{18}O_{V\text{-}SMOW}$ values (Fig. 12A, B). The international standard of carbon and oxygen isotope is NBS-20 (limestone, Solenhofen, Germany), and its recommended values are –1.06‰ and 26.64‰ for $\delta^{13}C_{V\text{-}PDB}$ and $\delta^{18}O_{V\text{-}SMOW}$, respectively. The minimum volume required for accurate measurements is c. 2 mg of calcite. In the case of graphite, the average of $\delta^{13}C_{V\text{-}PDB}$ values for NBS-21 is –28.24 ± 0.03‰ (1σ; n = 9) and its recommended values is –28.1‰. The minimum volume required for accurate measurement is c. 20 μg (Fig. 12C). The results for

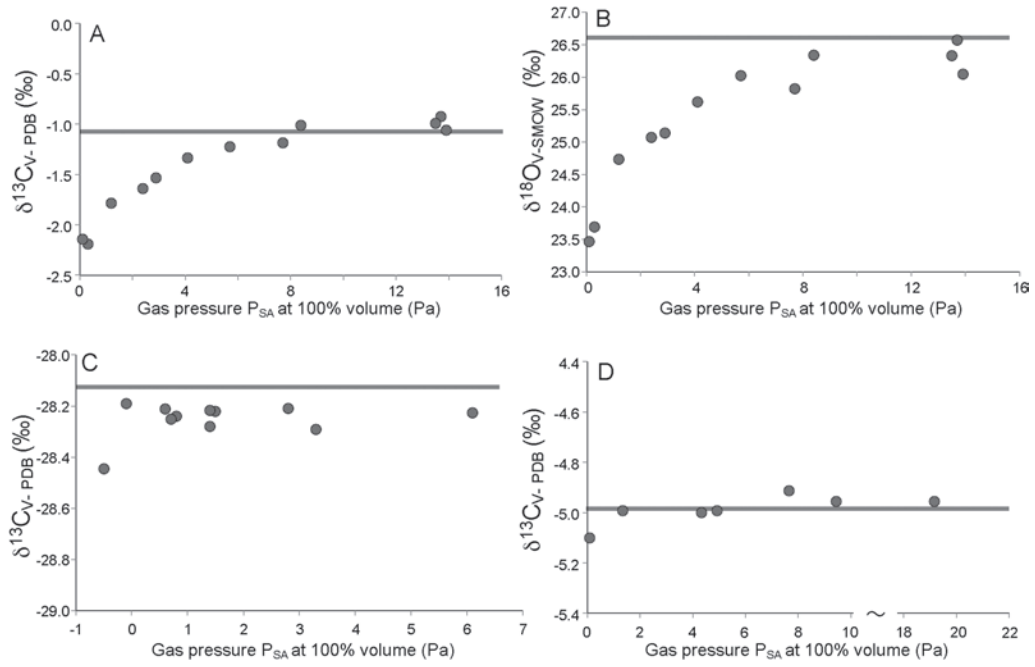

Fig. 12. The results of carbon and oxygen isotope measurements of international standards and a laboratory diamond standard. A) $\delta^{13}C_{V\text{-}PDB}$ values of NBS-20 limestone plotted against gas pressure (P_{SA}) at maximum volume of sample reservoir. B) $\delta^{18}O_{V\text{-}SMOW}$ values of NBS-20 limestone plotted against gas pressure (P_{SA}) at maximum volume of sample reservoir. C) The $\delta^{13}C_{V\text{-}PDB}$ results of NBS-21 graphite powder plotted against gas pressure (P_{SA}) at maximum volume of sample reservoir. D) The $\delta^{13}C_{V\text{-}PDB}$ results of laboratory diamond standard.

diamond analysis were also similar, with $\delta^{13}C_{V\text{-}PDB}$ values giving consistent results for both large volume (768 μg) and small volume samples (12.4 μg) –4.98 ± 0.06‰ (1 σ; n = 7) (Fig. 12D).

We also tested the carbon isotope measurements of laboratory standard graphite (SP1) using the micro-volume trap. The results show that carbon isotope measurements can be accurately done using MV trap (Fig. 13). However, measurements using MV-trap show considerable fractionation (>0.5) for oxygen isotopes due to rapid pressure decrease in the sample side during the measurement and hence it was concluded that small volumes of CO_2 gas can be measured accurately for both carbon and oxygen isotopes for the required precision using T_3 at a lower output of c. 500 mV and further experiments are required to use the MV trap of simultaneous measurements of carbon and oxygen isotopes.

Concluding remarks

A new inlet vacuum system was built and connected to the MAT-253 mass spectrometer

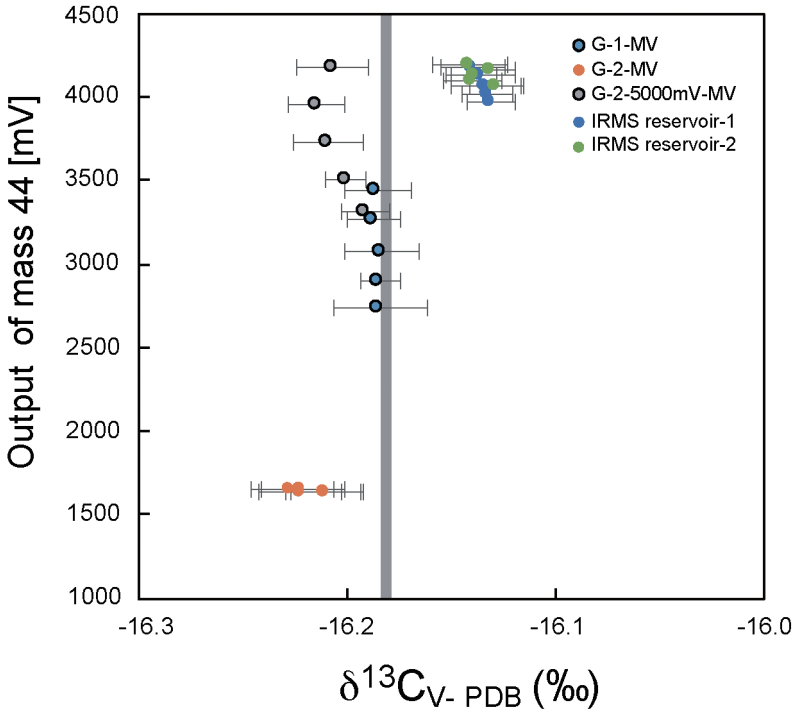

Fig. 13. The results of carbon isotope measurements of laboratory graphite standard (SP1) using the newly set up micro-volume trap. Note the vertical axis is the output of mass 44.

for the preparation and analyses of carbon and oxygen isotopes using CO_2 gas. The vacuum line holds high vacuum for time intervals required for a single session of measurements spanning for >12 hours. A minimum volume c. 2 milligram of calcite is required for the precise measurement carbon and oxygen isotopes, whereas c. 12 micrograms of pure carbon (graphite or diamond) is required for the precise measurement of carbon isotopes.

Acknowledgements

This study was supported by the Grant-in-Aid for Scientific Research on Innovative Areas (No. JP15H05831) to M S-K from the Ministry of Education, Culture, Sports, Science and Technology, Japan (MEXT). SK acknowledge a research associateship and a fellowship for doctoral program from Niigata University. We thank constructive comments by Watanabe Naoki (Research Institute for Natural Hazards and Disaster Recovery, Niigata University) and editorial comments by Matsuoka Atsushi (Faculty of Science, Niigata University).

References

Bowen, R., 1966, Paleotemperature analysis. *Elsevier Series Vol. 2: Methods in geochemistry and geophysics*, 265 p.

Coplen, T. B., 1988, Normalization of oxygen and hydrogen isotope data. *Chem. Geol.*, **72**, 293–297.

Coplen, T. B., 1994, Reporting of stable hydrogen, carbon, and oxygen isotopic abundances. *Pure Appl. Chem.* **66**, 273–276.

Coplen, T. B., 1996, New guidelines for reporting stable hydrogen, carbon, and oxygen isotope-ratio data. *Geochim. Cosmochim. Acta*, **60**, 3359–3360

Coplen, T.B., Kendall, C. and Hopple, J., 1983, Comparison of stable isotope reference samples. *Nature*, **302**, 236–238.

Cornides, J. and Kusakabe, M., 1977, Preparation of carbon dioxide from magnesite for isotopic analysis. *Fresenius Z. Anal. Chem.* **287**, 310–311.

Craig, H., 1957. Isotopic standards for carbon and oxygen and correction factors for mass spectrometric analysis of carbon dioxide. *Geochim. Cosmochim. Acta*, **12**, 133–149.

Hoefs, J., 1997, Stable Isotope Geochemistry, Springer, Berlin, 201p.

Nier, A.O., 1947. A mass spectrometer for isotope and gas analysis. *Rev. Sci. Instrum.*, **18**, 398–411.

Northrop, D. A. and Clayton, R. N., 1966, Oxygen-isotope fractionations in systems containing dolomite. *J. Geol.*, **74**, 174–196.

Rosenbaum, J. and Sheppard, S. M. F., 1986, An isotopic study of siderites, dolomites and ankerites at high temperatures. *Geochim. Cosmochim. Acta*, **50**, 1147–1150.

Sharma, T. and Clayton, R. N., 1965, Measurement of O^{18}/O^{16} ratios of total oxygen of carbonates. *Geochim. Cosmochim. Acta*, **29**, 1347–1353.

Wada, H., Niitsuma, N. and Saito, T., 1982, Carbon and oxygen isotopic measurements of ultra-small samples. *Geosci. Rep. Shiz. Univ.*, **7**, 35–50.

Wada, H., Fujii, N. and Niitsuma, N., 1984a, Analytical method of stable isotope for ultra-small amount of carbon dioxide with MAT250 mass-spectrometer. *Geosci. Rep. Shiz. Univ.*, **10**, 103–112.

Wada, H., Itoh, R. and Akiyama, F., 1984b, Preparation and measurement of carbon dioxide for stable isotope analysis of small-amount of graphite. *Geosci. Rep. Shiz. Univ.*, **10**, 133–141.

Wada, H., Okuda, K., Osada, Y., Nagao, H., Akutsu, S., Hamamatsu ,T., Satish-Kumar, M. and Niitsuma, N., 2008, Carbon and oxygen isotopic measurement using MAT-251 mass-spectrometer at Shizuoka University. *Geosci. Rep. Shiz. Univ.*, **35**, 29–43.

Wada, H. and Itoh, R., 1990, Stable isotope analysis of small amount of carbon dioxide and its application to the micro scale zoning of graphite crystals in metamorphic rocks. *Mass Spectr.*, **38**, 287–294.

Table 1. Carbon and oxygen isotope results of laboratory standard CO_2 gas for one year starting from April, 2020 to March 2021.

Measurement date	[44] signal (mV)	$\delta^{13}C$ (‰)	1σ	$\delta^{18}O$ (‰)	1σ
20200403-F	2074	-29.773	0.028	3.991	0.027
20200406-F	2246	-29.749	0.040	3.983	0.025
20200406-F	2202	-29.820	0.016	3.899	0.028
20200626-S	2127	-29.794	0.038	3.973	0.025
20200627-S	2134	-29.801	0.021	3.944	0.035
20200628-S	2105	-29.838	0.012	3.898	0.031
20200722-F	1378	-29.787	0.049	4.000	0.111
20200723-S	977	-29.814	0.054	3.987	0.108
20200723-F	796	-29.801	0.070	3.961	0.180
20200916-S	1793	-29.763	0.031	4.057	0.033
20200916-F	1890	-29.762	0.019	4.027	0.041
20200920-F	2193	-29.809	0.014	4.004	0.021
20201017-S	2162	-29.876	0.032	3.950	0.037
20201021-S	2069	-29.877	0.003	3.885	0.056
20201105-S	1514	-29.879	0.038	3.998	0.019
20201112-S	1453	-29.897	0.033	3.845	0.010
20201112-F	2157	-29.815	0.010	4.016	0.043
20201121-S	1411	-29.768	0.034	4.030	0.050
20201215-S	1997	-29.815	0.107	3.903	0.183
20201217-S	1178	-29.795	0.026	3.999	0.070
20201218-S	1060	-29.786	0.042	3.969	0.050
20210114-S	1606	-29.761	0.018	3.934	0.101
20210115-S	1037	-29.862	0.037	3.797	0.090
20210118-S	1538	-29.763	0.025	4.014	0.050
20210120-S	1544	-29.816	0.012	3.949	0.040
20210121-S	1518	-29.858	0.036	3.822	0.037
20210122-S	1524	-29.752	0.052	4.011	0.060
20210123-S	1504	-29.783	0.020	3.989	0.021
20210125-S	1462	-29.772	0.017	4.003	0.013
20210126-S	1465	-29.783	0.027	3.994	0.055
20210213-S	1520	-29.772	0.034	4.025	0.028
20210213-F	1416	-29.777	0.020	3.923	0.040
20210214-S	1503	-29.818	0.017	3.915	0.028
20210218-S	1453	-29.762	0.025	4.020	0.039
20210218-F	1347	-29.798	0.011	3.928	0.060
20210219-S	1232	-29.780	0.038	4.046	0.045
20210219-F	1376	-29.737	0.024	4.015	0.046
20210314-S	1694	-29.741	0.025	4.047	0.020
20210315-S	1622	-29.755	0.020	4.032	0.033
20210326-S	1356	-29.723	0.035	4.049	0.038
20210326-F	1371	-29.782	0.030	3.974	0.063
20210402-S	1193	-29.764	0.029	4.051	0.043
20210402-F	1154	-29.810	0.018	3.953	0.046
20210405-S	1163	-29.850	0.016	3.917	0.028
Average and standard deviation		-29.796	0.041	3.971	0.062

Table 2. Carbon and oxygen isotope results of NIST NBS-20 limestone, NBS-21 graphite and NU-Diamond.

Sample	Weight	PSA @ VSA100	$\delta^{13}C$ (‰)	1σ	$\delta^{18}O$ (‰)	1σ
NBS-20 limestone	(in mg)					
MSTD-S			-29.755	0.020	4.032	0.033
NBS-20-1		13.9	-1.060	0.010	26.050	0.010
NBS-20-2	2.9436	13.7	-0.924	0.011	26.574	0.020
NBS-20-3		13.5	-0.990	0.010	26.331	0.040
NBS-20-4	2.1572	7.7	-1.184	0.026	25.821	0.037
NBS-20-5	1.9664	8.4	-1.012	0.016	26.342	0.070
NBS-20-6	1.5356	5.7	-1.226	0.013	26.028	0.052
NBS-20-7	0.9903	4.1	-1.334	0.016	25.624	0.058
NBS-20-8	0.8171	2.9	-1.533	0.023	25.138	0.068
NBS-20-9	0.7681	2.4	-1.639	0.031	25.070	0.031
NBS-20-10	0.4901	1.2	-1.782	0.034	24.737	0.039
NBS-20-11	0.2357	0.3	-2.189	0.031	23.694	0.076
NBS-20-12	0.1640	0.1	-2.142	0.047	23.470	0.066
MSTD-F			-29.865	0.007	3.761	0.020
Average of 1-5 measurements			-1.034	0.097	26.224	0.292
Recommended values			-1.060		26.640	
NBS-21 graphite	(in μg)	PSA @ VSA100				
MSTD-S			-29.741	0.025	4.047	0.020
NBS-21-1	120.9	6.1	-28.227	0.015		
NBS-21-2	66.5	3.3	-28.292	0.017		
NBS-21-3	58.2	2.8	-28.208	0.025		
NBS-21-4	47.1	1.5	-28.220	0.020		
NBS-21-5	45.5	1.4	-28.280	0.020		
NBS-21-6	44.7	0.8	-28.240	0.031		
NBS-21-7	43.4	0.6	-28.210	0.090		
NBS-21-8	33.1	1.4	-28.216	0.063		
NBS-21-9	24.7	0.7	-28.250	0.048		
NBS-21-10	9.4	0.1	-30.310	0.110		
NBS-21-11	7.0	-0.1	-28.190	0.014		
NBS-21-12	1.1	-0.5	-28.446	0.042		
MSTD-F			-29.814	0.018	3.729	0.027
Average of 1-9 measurement			-28.238	0.030		
Recommended value			-28.10			
NU-Diamond	(in μg)	PSA @ VSA100				
MSTD-S			-29.764	0.031	4.040	0.020
NU-Dia-1	768.4	19.2	-4.935	0.010		
NU-Dia-2	132.3	9.7	-4.952	0.020		
NU-Dia-3	106.2	7.8	-4.904	0.009		
NU-Dia-4	68.4	4.9	-4.984	0.026		
NU-Dia-5	64.4	4.1	-5.012	0.016		
NU-Dia-6	26.1	1.5	-4.988	0.049		
NU-Dia-7	12.4	0.1	-5.101	0.046		
MSTD-F			-29.895	0.025	3.745	0.025
Average of 1-9 measurement			-4.982	0.064		

Appendix-1. Step-by-step procedure for carbon and oxygen isotope measurements using the new inlet system of the Thermo Fischer Scientific MAT-253 isotope ratio mass spectrometer at Niigata University. Procedure for start up, inlet of reference CO_2 gas (WSTD IN), laboratory standard measurement in the beginning (MSTD start), carbonate sample measurement, graphite/diamond measurement, laboratory standard measurement in the end (MSTD final), returning back of reference CO_2 gas to the storage reservoir (WSTD Back), close down of the inlet system and changing phosphoric acid in the carbonate reaction system are given in order.

1	Start Up Preperation
2	Date = ?
3	Room Temperature =?
4	HV=?
5	Vac=?
6	Magnet Steps=?
7	Box=?
8	Trap=?
9	Turbo Pumps RPM=?
10	PST at 100=?
11	PSA at 100=?
12	PR=?
13	PL=?

1	WSTD IN
2	PL=?
3	Close Valve 15
4	Close Valve 16
5	Close Valve 17
6	Close Valve 18
7	Close Valve 19
8	Close Valve 20
9	Close Valve 21
10	Close Valve 22
11	Close Valve 13
12	Close Valve 6
13	Close Valve 2
14	Close Valve 3
15	Close Valve 4
16	Close Valve 8
17	Close Valve 9
18	Close Valve 10
19	PL=?
20	VST to 20
21	Open Valve 14
22	Open valve 12
23	Open valve 25
24	PL=?
25	Wait 1 Minute
26	Close Valve 12
27	Set Liquid N2 on T5
28	Wait 5 minutes
29	PL=?
30	Close Valve 25
31	Open valve 21
32	PL=?
33	PST at 20=?
34	VST to 100
35	PST at 100=?
36	Open Valve 11
37	Open Valve B
38	[45]ST=?
39	Peak Centre check
40	Auto Focus
41	[45]ST=?
42	Pass to Gas Configuration

1	MSTD Start Measurement
2	PL=?
3	Open Valve 27
4	PL=?
5	Close Valve 27
6	Close Valve 21
7	PL=?
8	Open Valve 26
9	Wait 1 Minute
10	Close Valve 26
11	Open Valve 14
12	Open Valve 6
13	Open Valve 4
14	Open Valve 10
15	Open Valve 27
16	PL=?
17	Wait 1 Minute
18	Close Valve 14
19	Close Valve 6
20	Close Valve 4
21	PSA at 100=?
22	[45] SA = [45] ST ?
23	Measurement
24	Open Valve 21
25	PL=?

1	Carbonate Measurement
2	PR=?
3	Close Valve M20
4	Drop Thimble to Reaction Vessel
5	Wait 10 Minutes
6	T2> -126, Cool Pentane Trap
7	Open Valve 18
8	Open Valve 17
9	Close Valve 19
10	PR=?
11	Set Liquid N2 at T1
12	Open Valve M20
13	PR=?
14	Wait 10 Minutes
15	Close Valve M20
16	Open Valve 19
17	PR=?
18	Close Valve 17
19	Close Valve 18
20	Close Valve 19
21	Set Liquid N2 at T3
22	Open Valve 15
23	Open Valve 16
24	Open Valve 7
25	Open Valve 8
26	Remove Liquid N2 at T1
27	Defrost Trapped CO2 at T1
28	PR=?
29	Wait for 5 Minutes
30	Pr=?
31	Close Valve 7
32	Open Valve 9
33	Defrost Trapped CO2 at T3
34	PSA at 100=?
35	Close Valve 9
36	Adjust VSA
37	[45] SA = [45] ST ?
38	Measurement
39	After Measurement, VSA to 100
40	Open Valve 2
41	Open Valve 4
42	Open Valve 3
43	PSA at 100=?
44	Open Valve M20
45	Open Valve 19
46	Stir the Reaction Vessel
47	Wait 5 Minutes
48	Close Valve M20
49	Drop Next Thimble
50	Repeat the steps

1	Graphite/Diamod Measurement Start
2	PR=?
3	Open Valve 19
4	Set Tube Sample
5	Open Valve M21 Slowly
6	Wait 5 Minutes
7	Close Valve 19
8	Open Valve 18
9	Open Valve 17
10	Wait 1 Minute
11	PR=?
12	T2> -126, Cool Pentane Trap
13	Set Liquid N2 at T1
14	Crack Sample Tube
15	PR Maximum=?
16	PR Minimum=?
17	Wait 5 Minutes
18	PR=?
19	Close Valve M21
20	Open Valve 19
21	PR=?
22	Close Valve 17
23	Close Valve 18
24	Close Valve 19
25	Set Liquid N2 at T3
26	Open Valve 15
27	Open Valve 16
28	Open Valve 7
29	Open Valve 8
30	Remove Liquid N2 at T1
31	Defrost Trapped CO2 at T1
32	PR=?
33	Wait for 5 Minutes
34	Pr=?
35	Close Valve 7
36	Open Valve 9
37	Defrost Trapped CO2 at T3
38	PSA at 100=?
39	Close Valve 9
40	Adjust VSA
41	[45] SA = [45] ST ?
42	Measurement
43	After Measurement, VSA to 100
44	Open Valve 2
45	Open Valve 4
46	Open Valve 3
47	PSA at 100=?
48	Set Next Tube Sample

1	MSTD Final Measurement
2	PL=?
3	Open Valve 27
4	PL=?
5	Close Valve 27
6	Close Valve 21
7	PL=?
8	Open Valve 26
9	Wait 1 Minute
10	Close Valve 26
11	Open Valve 14
12	Open Valve 6
13	Open Valve 4
14	Open Valve 10
15	Open Valve 27
16	PL=?
17	Wait 1 Minute
18	Close Valve 14
19	Close Valve 6
20	Close Valve 4
21	PSA at 100=?
22	[45] SA = [45] ST ?
23	Measurement
24	Open Valve 21
25	PL=?

1	WSTD Back
2	PL=?
3	Close all Valves
4	PL=?
5	Set Liquid N2 on T5
6	Open Valve 25
7	PL=?
8	Open Valve 12
9	Open Valve 14
10	PL=?
11	Wait 5 Minutes
12	PL=?
13	Close Valve 25
14	Open Valve 21
15	PL=?
16	WSTD Back Finish

1	Close Down
2	Open Valve 21
3	Open Valve 20
4	Open Valve 19
5	Open Valve 18
6	Open Valve 17
7	Open Valve 16
8	Open Valve 15
9	Open Valve 8
10	Open Valve 9
11	Open Valve 10
12	Open Valve 11
13	Open Valve 12
14	Open Valve 13
15	Open Valve 2
16	Open Valve 3
17	Open Valve 4
18	Close Valve 7
19	Close Valve 14

1	Phosphoric Acid Exchange
2	Close Valve M22
3	Lower Stage of Reaction Chamber rotating Anti-clockwise
4	Remove Oil Inlet Tubes
5	Open Sample Holder Lid
6	Rotate Ring Clockwise Near Neck of Reation Vessel
7	Replace Reaction Vessel
8	Rotate Ring Anti-Clockwise Near Neck of Reation Vessel
9	Fit the Oil Inlet Tubes
10	Raise Stage of Reaction Chamber rotating Clockwise
11	Close Sample Holder Lid
12	Open Valve M22
13	Open Valve 19
14	Open Valve M20 Slowly Looking at Turbo Pump
15	Wait 15 Minutes
16	Close Valve 19
17	Open Valve 18
18	Open Valve 17
19	Wait 1 Minute
20	PR=?
21	Start Carbonate Measurement

Carboniferous brachiopod *Latiproductus edelburgensis* (Phillips, 1836) from Akiyoshi and Omi, Japan

Yousuke IBARAKI*, Yasuhiro OTA** and Masayuki FUJIKAWA***

Abstract

A productid brachiopod species, *Latiproductus edelburgensis* (Phillips), is described from the upper Visean to lower Serpukhovian of the Akiyoshi Limestone, Akiyoshi, southwest Japan and the Omi Limestone, Omi, central Japan. The occurrence of *L. edelburgensis* indicates a late Visean to early Serpukhovian age for the *Mediocris mediocris* Zone of the Akiyoshi Limestone and the *Eostaffella–Millerella* Zone of the Omi Limestone. The stratigraphic and geographic distributions of *L. edelburgensis* are restricted to the Lower Carboniferous (upper Visean to lower Serpukhovian) of Europe, central and eastern Asia, northern Africa and western Panthalassa, and completely absent in North and South America and Australia.

Key words: Akiyoshi, Brachiopoda, *Latiproductus edelburgensis*, lower Carboniferous, Omi.

Introduction

Gigantoproductoids are large-sized brachiopods known as a leading fossil of Early Carboniferous (late Visean–early Serpukhovian) from Europe, Algeria, Russia, China and North America. In Japan, several gigantoproductoid species were previously described from the Omi Limestone in Omi, Itoigawa City, central Japan (Hayasaka, 1924), the Akiyoshi Limestone in Akiyoshi Plateau, southwest Japan (Yanagida, 1979), the Koyama Limestone in Oga, Takahashi City, southwest Japan (Ibaraki et al., 2014), the Ichinotani Formation in the Fukuji area, Hida Mountains (Tazawa and Kato, 1986; Ibaraki et al., 2009), the Tsuchikurazawa

* Fossa Magna Museum, Itoigawa 941-0056, Japan
** Kitakyushu Museum of Natural History and Human History, Kitakyushu 805-0071, Japan
*** Akiyoshidai Science Museum, Mine 754-0511, Japan
Corresponding author: Yousuke Ibaraki,
yousuke.ibaraki@city.itoigawa.lg.jp
(Manuscript received 1 March, 2021; accepted 20 March, 2021)

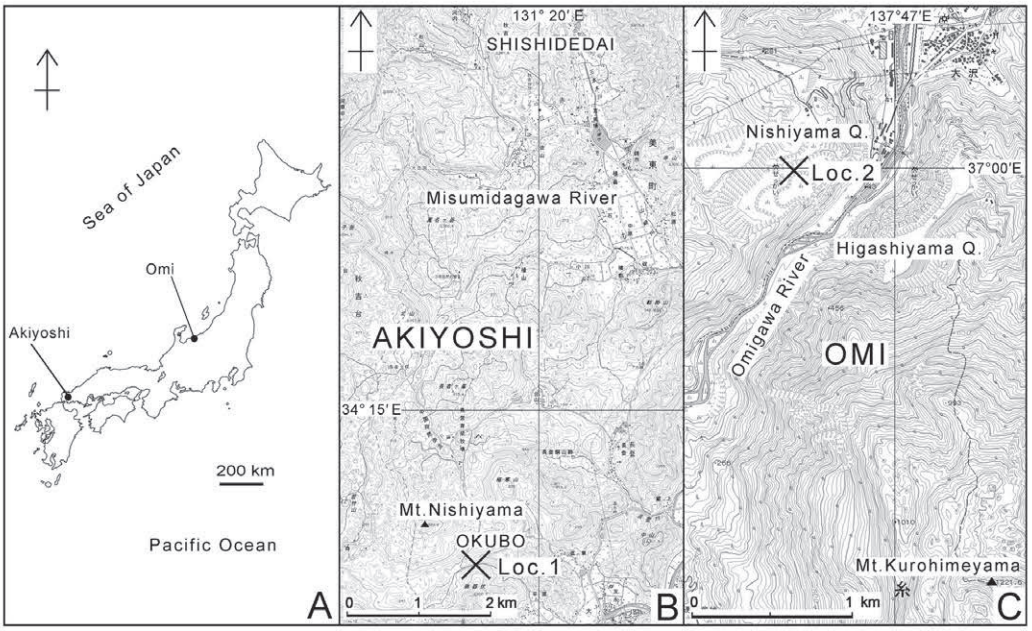

Fig. 1. Map showing the fossil localities, Loc. 1 (Okubo), Loc. 2 (Nishiyama Quarry), A: Akiyoshi, B: Omi, using the topographical map of "Akiyoshidaihokubu", "Akiyoshidai" and "Itoigawa" scale 1:25,000 published by the Geographical Survey Institute of Japan.

Limestone in Kotaki, Itoigawa City, central Japan (Tazawa, 2004; Ibaraki et al., 2008, 2010) and the Onimaru Formation in the Nagaiwa-Onimaru area and the Hikoroichi Formation in the Hikoroichi area, southern Kitakami Mountains, northeast Japan (Tazawa and Miyake, 2002; Tazawa and Ibaraki, 2009; Tazawa, 2018; Tazawa and Taira, 2020).

In this paper, we examine four specimens of gigantoproductoids from the *Mediocris mediocris* Zone of the Akiyoshi Limestone in Shishidedai and Okubo, Akiyoshi Plateau, southwest Japan and the *Eostaffella–Millerella* Zone of the Omi Limestone in Nishiyama Quarry, Omi, Itoigawa City, central Japan (Fig. 1).

Material

The Akiyoshi specimens were collected by late Professor Juichi Yanagida of Kyushu University. Most of the Omi specimens were collected by Emeritus Professor Jun-ichi Tazawa of Niigata University. Based on the present systematic descriptions, all of the specimens are referred to *Latiproductus edelburgensis* (Phillips, 1836), originally described from the Lower Carboniferous of Bolland, Lancashire, England, the UK.

The specimens described herein are registered and housed in the Fossa Magna Museum

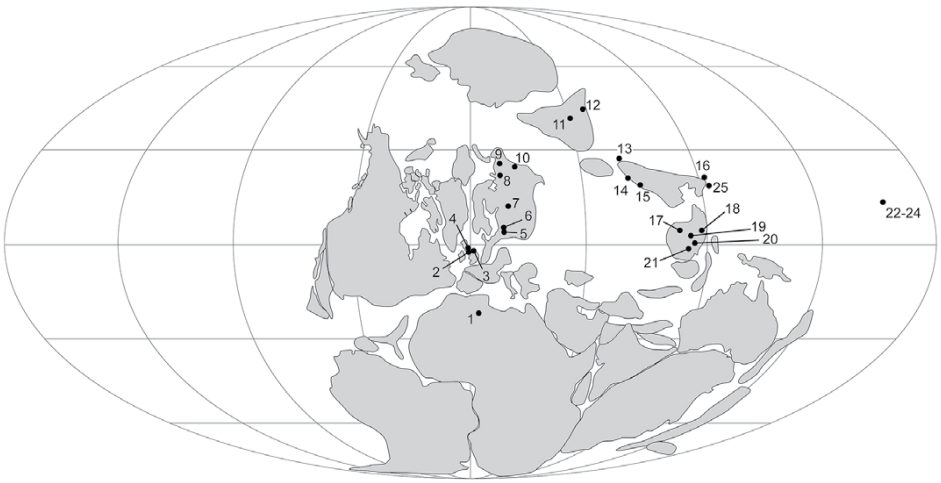

Fig. 2. Geographical distribution of *Latiproductus edelburgensis* (Phillips) in the late Visean (adapted Scotese, 2004). 1: Algeria, 2: Lancashire, 3: Yorkshire, 4: Pennine Mountains, 5: Silesia, 6: Holy Cross Mountains, 7: Moscow Basin, 8: northern Timan 9: Pechora, 10: central Ural, 11: central Kazakhstan, 12: northern Kirgizia, 13: Tien-Shan, 14: Xizang 15: Qinghai, 16: Jilin, 17: Sichuan, 18: Jiangxi, 19: Hubei, 20: Hunan, 21: Guizhou, 22: Akiyoshi, 23: Omi, 24: Oga, 25: Nagaiwa-Onimaru.

(specimen numbers prefixed with FMM) and the Kitakyushu Museum of Natural History and Human History (specimen numbers prefixed with KMNHIvP).

Stratigraphic and geographic distributions of *Latiproductus edelburgensis*

Latiproductus edelburgensis has been described from the upper Visean–Serpukhovian of Algeria (1; Legrand-Brain, 1973, 1980; Pareyn, 1961). Lancashire, England (2; Phillips, 1836), Yorkshire, England (3; Davidson, 1958–1963; Prentice, 1956), Pennine Mountains, England (4; Pattison, 1981), Silesia, Germany (5; Paeckelmann, 1931), Holy Cross Mountains, Poland (6; Zakowa, 1986), Moscow Basin, western Russia (7, Sarytcheva and Sokolskaya, 1952), northern Timan, western Russia (8; Aisenberg and Poletaev, 1970), Pechora, western Russia (9; Kalashnikov, 1974), central Urals, western Russia (10; Einor, 1957), central Kazakhstan (11; Litovinovich, Aksenova and Razina, 1969), northern Kirgizia (12; Gladchenko, 1955; Galitzkaja, 1977), Tien-Shan, Northwest China (13; Gröber, P., 1909; Krenkel, 1913), Xizang, Southwest China (14; Jin et al., 1985), Qinghai, Northwest China (15; Yang et al., 1962), Jilin, Northeast China (16; Lee et al., 1980), Sichuan, Southwest China (17; Yang and Jiang, 1987), Jiangxi, South China, (18; Wang et al., 1982), Hubei, South China (19; Wang, 1984), Hunan, South China (20; Tan, 1987; Liu et al., 1982), Guizhou, South China (21; Chao, 1927), Akiyoshi, southwest Japan (22; Yanagida, 1989), Omi, central Japan (23; This paper), Oga, southwest Japan (24: Ibaraki et al., 2014), Nagaiwa-Onimaru, South Kitakami Mountains, northeast Japan (25; Tazawa and

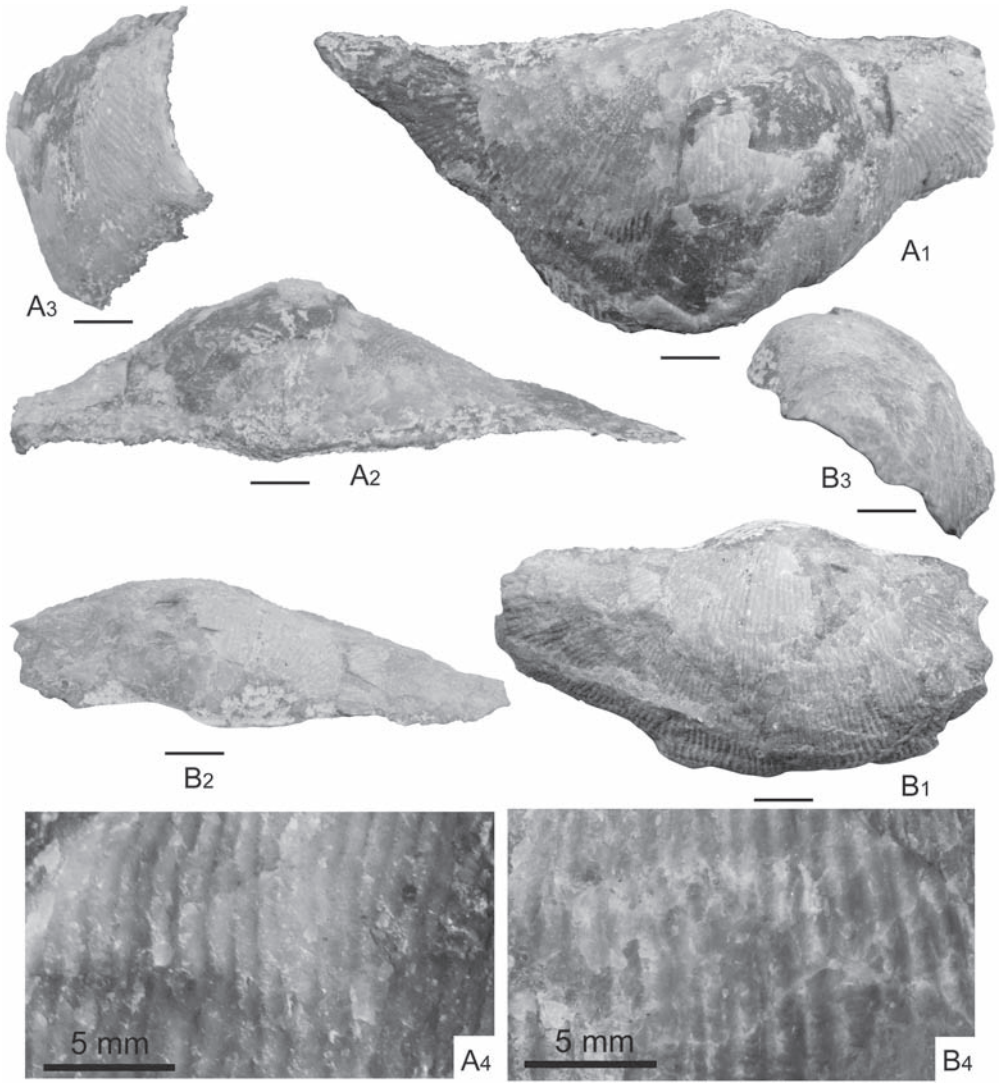

Fig. 3. A1 – A4: ventral, posterior, lateral views and enlarged radial costae of conjoined valve, KMNHIv710001. B1 – B4: ventral, posterior, lateral views and enlarged radial costae of dorsal valve, KMNHIv710002. Scale bars are 1 cm, expect of A4 and B4.

Taira, 2020) (Fig. 2).

From the above data, the range of *Latiproductus edelburgensis* is assigned to late Visean–Serpukhovian, which is the same as the summary by Brunton et al. (2000). Qiao and Shen (2015) also concluded as above. Palaeobiogeographically, it is noteworthy that *L. edelburgensis* has been mostly found from equatorial to mid latitude areas of Asia and Europe, but completely absent in North America, South America and Australia. This result is consistent with one of the conclusions in Qiao and Shen (2014). The lower Carboniferous

limestones of Omi and Akiyoshi were probably reef-seamount of the Panthalassa in the mid-latitude area of the Northern Hemisphere during late Visean–Serpukhovian. This conclusion is consistent with that of Tazawa et al. (2005), in which they noted that the Akiyoshi-Omi reef-seamounts were probably located at the lower to middle northern palaeolatitude on the Panthalassa during the early Carboniferous (late Visean).

Systematic descriptions

(by Y. Ibaraki)

Order Procuctida Sarycheva and Sokolskaya, 1959
Suborder Productidina Waagen, 1883
Superfamily Linoproductoidea Stehli, 1954
Family Linoproductidae Stehli, 1954
Subfamily Gigantoproductinae Muir-Wood and Cooper, 1960
Tribe Semiplanini Sarycheva, 1960
Genus *Latiproductus* Sarycheva and Legrand-Blain, 1977

Type species.—*Productus latissimus* Sowerby, 1822.

Latiproductus edelburgensis (Phillips, 1836)
Figs. 3–4

Producta edelburgensis Phillips, 1836, p. 214, pl. 7, fig. 5.
Productus giganteus mut. *edelburgensis* (Phillips). Glöber, 1909, p. 372, pl. 1, fig. 11; pl. 2, figs. 3–4.
Productus giganteus var. *edelburgensis* (Phillips). Hayasaka, 1924, p. 143, pl. 54, figs. 1, 2.
Striatifera edelburgensis (Phillips). Chao, 1927, p. 107, pl. 10, figs. 4, 5; pl. 12, fig. 6.
Gigantella edelburgensis var. *glöberi* Sarycheva, 1928, p. 51, pl. 4, fig. 5.
Productus (*Gigantella*)? *edelburgensis* (Phillips). Paeckelmann, 1931, p. 260, pl. 29, figs. 1a–1c.
Productus (*Gigantella*) *edelburgensis*? Ozaki, 1939, p. 244, pl. 38, fig. 2.
Productus (*Gigantella*) *edelburgensis*? var. *shajenwaensis* Ozaki, 1939, p. 242, pl. 37, fig. 4; pl. 38, fig. 1; pl. 39, fig. 2.
Gigantoproductus edelburgensis (Phillips). Sarycheva in Sarycheva and Sokolskaya, 1952, p. 131, pl. 35, fig. 180; Prentice, 1956, p. 234, pl. 20, figs. 1a–c, 2; Galitskaya, 1977, p. 147, pl. 61, figs. 2a–2b; pl. 62, fig. 1; pl. 63, figs. 1–2.
Productus (*Gigantoproductus*) *edelburgensis* (Phillips). Gladchenko, 1955, p. 19, pl. 10, figs. 1a–1c.
Productus (*Gigantoproductus*) *edelburgensis* var. *schaitankaensis* Einor, 1957, p. 151. pl. 3, fig. 3.
Productus-Gigantoproductus-edelburgensis (Phillips). Pareyn, 1961, p. 202, pl. 24, figs. 4, 5.

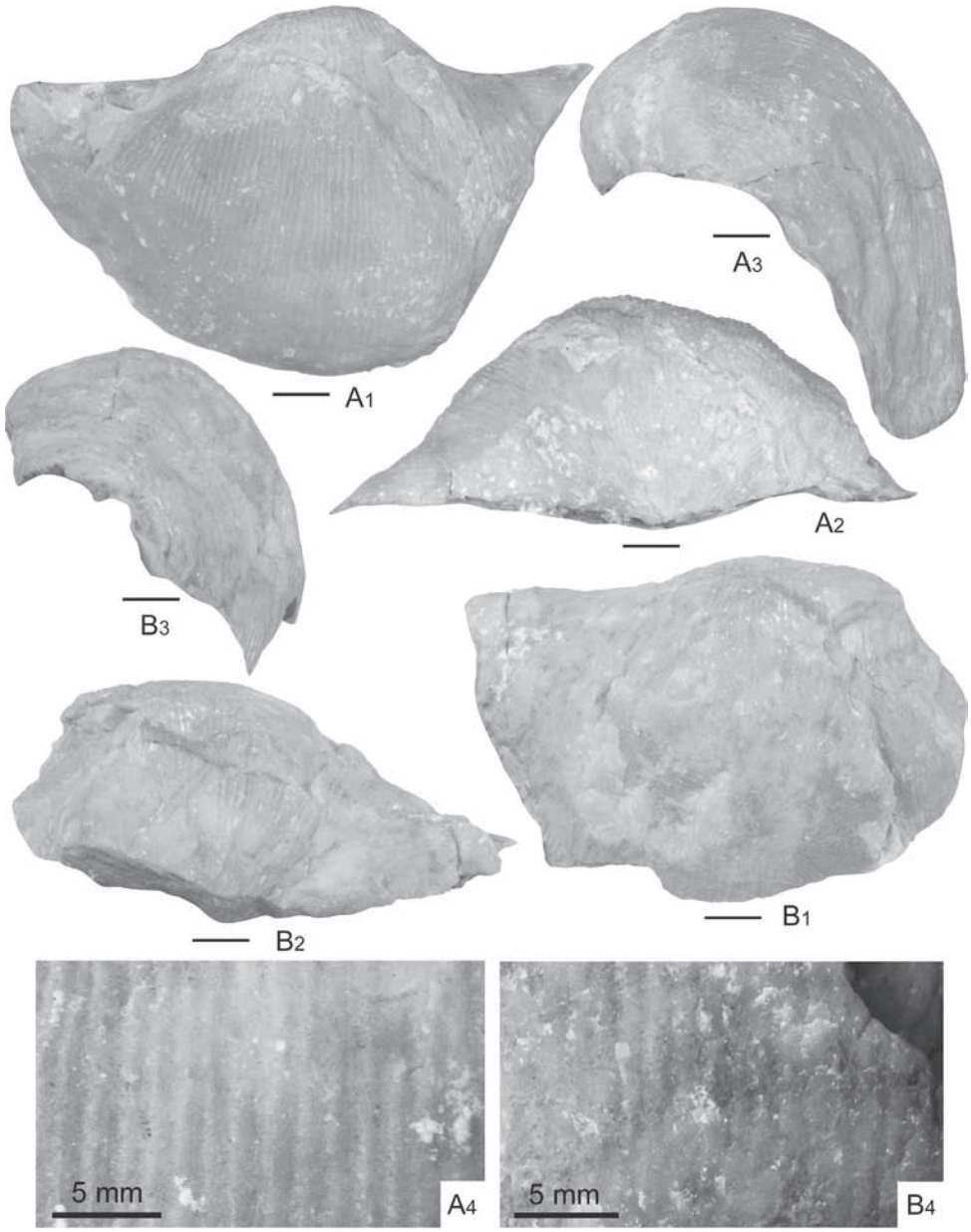

Fig. 4. A1 – A4: ventral, posterior, lateral views and enlarged radial costae of ventral valve, FMM2023. B1 – B4: ventral, posterior, lateral views and enlarged radial costae of ventral valve, FMM2024. Scale bars are 1 cm, expect of A4 and B4.

Productus (*Gigantoproductus*) *edelburgensis* var. *beleutensis* Litvinovich, 1962, p. 207. pl. 7, fig. 2.

Gigantoproductus cf. *edelburgensis* (Phillips). Legrand-Blain, 1973, p. 91, pl. 2, figs. 1a–1b.

Gigantoproductus edelburgensis edelburgensis (Phillips). Semichatova, 1975, p. 173, pl. 77, fig. 1.

Gigantoproductus edelburgensis schaitakaensis (Einor). Semichatova, 1975, p. 173, pl. 77, fig. 2.

Gigantoproductus edelburgensis? var. *shajenwaensis* (Ozaki). Yang et al., 1977, p. 368, pl. 146, fig. 4.

Gigantoproductus aff. *edelburgensis* (Phillips). Yanagida, 1979, p. 112, fig. 3.

Gigantoproductus aff. *submaximus* (Bolkhovitinova). Yanagida, 1979, p. 111, fig. 2.

Gigantoproductus edelburgensis var. *shajenwaensis* (Ozaki). Liu et al., 1982, p. 189; pl. 135, fig. 5.

Latiproductus (?) *edelburgensis sahariensis* forme a Legrand-Blain, 1980, p. 42, pl. 3, figs. 3; text-figs. 13, 15.

Latiproductus (?) *edelburgensis sahariensis* forme c Legrand-Blain, 1980, p. 46, pl. 5, figs. 1, 2; text-figs. 13, 16.

Latiproductus (?) *edelburgensis subsahariensis*. Legrand-Blain, 1980, p. 47, pl. 1, fig. 6; pl. 3, fig. 4; text-figs. 14, 17.

Latiproductus edelburgensis (Phillips). Zakowa, 1986, p. 65, pl. 6, fig. 1; Ibaraki et al., 2014, p. 17, fig. 3; Tazawa and Taira, 2020, p. 21, fig. 7.

Material.—(1) An imperfect conjoined valve, KMNHIv710001 from Loc. 1; (2) two ventral valves, FMM2023, 2024 from Loc. 2; (3) a dorsal valve, KMNHIv710002 from Loc. 1.

Description.—Shell medium size for genus, transversely semicircular in outline, with greatest width at hinge; length 60 mm, width 110 mm in the largest specimen (FMM2023); length 50 mm, width about 90 mm in the smallest specimen (FMM2024). Ventral valve moderately convex in lateral profile, strongly geniculated at 40－50 mm from umbo; flanks gently inclined; umbo small, rounded and inflated; ears large, triangular and moderately demarcated from flanks; sulcus absent. External surface of ventral valve ornamented with numerous costae but no rugae; costae regular in anterior part, but irregular in trail, numbering 8－10 per 10 mm at about midvalve, and costae sometimes bifurcated or inserted in anterior regions; intercostal sulci as wide as costae; several radial fluting crossing costae on trail; numerous fine growth lines on valve; spines or spine bases not preserved on the surface of valves. Dorsal valve slightly concave, geniculated at 40－50 mm from umbo; incurve of midvalve weaker than that of ventral valve; external surface of dorsal disc ornamented with numerous costae; costae regular, numbering 8－9 per 10 mm at about midvalve; costae sometimes bifurcated or inserted in anterior regions; no rugae; numerous fine growth lines over the inner surface; interior of both valves not observed.

Remarks.—The specimens are assigned to *Latiproductus edelburgensis* (Phillips, 1836), originally described from the Lower Carboniferous of Bolland, Lancashire, England, from account of size, shape, and external ornament of ventral valve, particularly in its size, shape of umbo. *Latiproductus latissimus* (Sowerby, 1822), described and figured by Pattison (1981) differs from *L. edelburgensis* in its smaller size and flattened ears, existence of a sulcus, finer costae, absence of intercostal sulci on ventral valve and thicker shell. *Gigantoproductus submaximus* (Bolkhovitinova, 1932) resembles *L. edelburgensis* in shape of ventral valve and

the presence of several rugae on trail, but differs in its larger size, finer costae on ventral valve. A specimen described as *Gigantoproductus* aff. *submaximus* (Bolkhovitinova) by Yanagida (1979) is reassigned to *Latiproductus edelburgensis*, owing to the following reasons: 1) The specimen of Yanagida (1979) lacks a long trail with fluting flexuously costae in the ventral valve, which are charasteristics of *L. edelburgensis* as shown in well-preserved specimen (Galitskaya, 1977: fig. 1, pl. 63) and 2) the ventral valve of *G. submaximus* is much larger and having finer costae than those of *L. edelburgensis*.

Acknowledgements

The first author extends cordially thank Jun-ichi Tazawa, Professor Emeritus Niigata University, for his earnest guidance and encouragement throughout the present study. We thank anonymous reviewers for critically reading the manuscript, by which this paper was greatly improved.

References

Aisenberg, D. E. and Poletaev, V. I., 1970, Brachiopoda. *In* Barkhatova, V. P., ed., *Carboniferous and Lower Permian biostratigraphy of northern Timan*. Nedra, Leningrad, 3–228 (in Russian).

Bolkhovitnova, M. A., 1932, New information of stratigraphy of Eugo-east part, general geological map, 58th sheet, Naucho-tech (ed.), Moskva, 49 p. (in Russian).

Brunton, C. H. C., Lazarev, S. S., Grant, R. E. and Jin, Y. G., 2000., Productidina. *In* Kaesler, R. L., ed., *Treatise on Invertebrate Paleontology, Part H Brachiopoda Revised, Volume 3: Linguliformea, Craniiformea and Rhynchonelliformea (Part)*, Geol. Soc. Amer., Boulder and Univ. Kansus, Lawrence, 424–609.

Chao, Y. T., 1927, Productidae of China. Part 1. Producti, *Palaeont. Sinica, Ser. B*, Fasc. 2, 83–120.

Davidson, T., 1858-1863, *British fossil Brachiopoda, Vol. **2**. Permian and Carboniferous species*. Palaeontograph. Soc., London, 280 p.

Einor, O. L., 1957, Carboniferous brachiopod fauna from the western slope in Central Ural. *Ezh. Vsesoy. Paleont. Obsch*, **16**, 142–161 (in Russian).

Galitskaya, A, Ya, 1977, *Early and Middle Carboniferous Productids from Northern Kyrgyzstan*. Ilim, Frunze, 297 p. (in Russian).

Gladchenko, A, Ya, 1955, *Field atlas of index fossils of Brachiopods from the lower Carboniferous of northern Kirgizia*. Akad. Nauk Kirgiz., SSR, Frunze, 30 p. (in Russian).

Glöber, P., 1909, Carbon und Carbonfossilien des nördlichen und zenttalen Tian-Schan. *Abh. König. Akad. Wissenschaft. 2 Klas.*, **24**, 341–384.

Hayasaka, I., 1924, On the fauna of anthracolithic limestone of Omi-mura in the western part of Echigo. *Sci. Rep. Tohoku Imp. Univ., 2nd Ser.*, **8**, 1–83.

Ibaraki, Y., Tazawa, J., Sato, K. and Nakamura, Y., 2008, *Gigantoproductus* (Carboniferous Brachiopoda) from Kotaki, Itoigawa City, Niigata Prefecture, central Japan. *Sci. Rep. Niigata Univ., (Geol.)*, no. 23, 55–64.

Ibaraki, Y., Tazawa, J. and Nakamura, Y., 2010, Additional *Gigantoproductus* species from the upper Visean-Namurian limestone of Kotaki, central Japan. *Sci. Rep. Niigata Univ., (Geol.)*, no. 25, 63–68.

Ibaraki, Y., Miyake, Y. and Tazawa, J., 2014, Early Carboniferous (late Visean) brachiopods from the Koyama Limestone of Kamiotake in the Oga area, Okayama Prefecture, Southwest Japan. *Earth Sci. (Chikyu Kagaku)*, **68**, 69–79.

Ibaraki, Y., Tazawa, J. and Miyake, Y., 2009, *Gigantoproductus* (Carboniferous Brachiopoda) from the lowest part of the Ichinotani Formation, Fukuji, Hida Gaien Belt, central Japan. *Sci. Rep. Niigata Univ., (Geol.)*, no. 24, 1–5.

Jin, Y., Wang, Y. Sun, D. and Shi, Q., 1985, Late Paleozoic and Triassic brachiopods from the East of the Quighan-Xizang Plateau. *In* Regional Geological Surveying Team of Sichuan Province and Nangjing Institute of Geology and Palaeontology, eds., *Stratigraphy and Palaeontology in W. Sichuan and E. Xizang, China (Part 3)*. Sichuan Sci. Tec. Press, Chengdu, 182–249 (in Chinese).

Kalashnikov, N. V., 1974, *Early Carboniferous brachiopod from Pechora Urals*. Nauka, Leningrad, 220 p. (in Russian).

Krenkel, E., 1913, Wissenschaftliche erbebnisse der Reise von Prof. Dr. G. Merzbacher im zentralen und östlichen Tian-Schan 1907/**8**. *Abh. Königlich Bayerischien Akad. Wissen. Math. –phys*., klasse 3, band. **8**, 1–44.

Lee, L., Gu, F. and Su, Y., 1980, Carboniferous and Permian Brachiopoda. *In* Shenyang Institute of Geology and Mineral Resources eds., *Paleontological Atlas of Northeast China, Paleozoic Volume*, Geol. Pub. House, Beijing, 327–428 (in Chinese).

Legrand-Blain, M., 1973, Les gigantoproductides (brachiopodes) du Sahara Algerien. *Bull. Soc. Hist. Natur. de l'Afrique du Nord*, **64**, 79–157.

Legrand-Blain, M., 1980, Les gigantoproductides (brachiopodes) du Sahara Algerien 3-Semiplanidae Viseens et Namuriens. *Bull. Soc. Hist. Natur. de l'Afrique du Nord*, **69**, 3–85.

Litvinovich, N. V., 1962, Carboniferous and Permian Deposits of the Western Part of Central Kazakhstan. Izd. Moskov. Univ., Moskva, 389 p. (in Russian).

Litvinovich, N. V., Aksenova, G. G. and Razina, T. P., 1969, *Stratigraphy and lithology of the Lower to Upper Carboniferous in central western part of Kazakhstan*. Nedra, Moskva, 447 p. (in Russian).

Liu, Z., Tan, Z. and Ding, Y., 1982, Brachiopoda. *In* Geological Bureau of Hunan eds., *Palaeontological Atlas of Hunan Province*. Geol. Pub. House, Beijing, 172–216 (in Chinese).

Muir-Wood, H. M. and Cooper, G. A., 1960, Morphology, classification and life habits of the Productoidea (Brachiopoda). *Geoli. Soc. America Mem*., **81**, 447 p.

Ozaki, K., 1939, On some Lower Carboniferous brachiopods from central Hunan, China. *Shanghai Sci. Inst. Jour. Section 2*, **2**, 225–282.

Paeckelmann, W., 1931, Die Fauna des deutschen Unterkarbons, 2 Teil. *Abhandl. Preus. Geol. Landesanstalt Neve Folge*, **136**, 440 p.

Pareyn, C., 1961, *Massifs carboniferes du Sahara Sud-Oranais, Tome 1, Publications du Centre de Recherches Sahariennes, serie geologie*, no. 1, Edit. Centre Nation. Recher. Scient., Paris, 202 p.

Pattison, J., 1981, The stratigraphical distribution of gigantoproductoid brachiopods in the Viséan and Namurian rocks of some areas in northern England. *Rep. Inst. Geol. Sci*., no. 81/9, 1–30.

Phillips, J., 1836, *Illustrations of the geology of Yorkshire; or a description of the strata and organic remains: accompanied by a geologic map, sections and diagrams and figures of the fossils, Part 2. The Mountain Limestone Districts*, John Murray, London, 253 p.

Prentice, J. E., 1956, *Gigantoproductus edelburgensis* (Phillips) and related species. *Proc. Yorkshire geol. Soc*., **30**, 229–258.

Qiao, L., and Shen, S.-Z., 2014, Global paleobiogeography of brachiopods during the Mississippian – Response to the global tectonic reconfiguration, ocean circulation, and climate changes. *Gondwana Res*., **26**, 1173–1185.

Qiao, L., and Shen, S.-Z., 2015, A global review of the Late Mississippian (Carboniferous) *Gigantoproductus* (Brachiopoda) faunas and the paleogeographical, paleoecological, and paleoclimatic implications. *Palaeogeogr. Palaeoclimat. Palaeoecol*., **420**, 128–137.

Sarycheva, T. G., 1928, Lower Moscovian Productids group *Productus giganteus* Mart. (*Gigantella* gen. nov.). *Tr. GNII.*, no. 1, 1–71 (in Russian).

Sarycheva, T. G., 1960, Order Productida. *In* Orlov, Y. A., ed., *Basic Paleontologii*, **7**, Akad. Nauk SSSR, Moscow, 221–238 (in Russian).

Sarycheva, T. G. and Legrand-Blain, M., 1977, Generic composition and evolution of the family Semiplanidae (Brachiopoda). *Paleont. Zhur*., 1977, no. 2, 70–82 (in Russian).

Sarycheva, T. G. and Sokolskaya, A. N., 1952, A description of the Paleozoic Brachiopoda of the Moscow Basin. *Tr. Paleont. Inst., Akad. Nauk SSSR*, **38**, 1–307 (in Russian).

Sarycheva, T. G. and Sokoloskaya, A. N., 1959, On the classification of pseudopuncutate brachiopods. *Dok. Akad. Nauk SSSR*, **125**, 181–184 (in Russian).

Semichatova, S, V., 1975, Brachiopoda. *In* Garanj, I. M., Guseva, S. N., Devingtal, V. V., Donakova, L. M.,

Enokyan, N. V., Kalashnikov, N. N., Semichatova, S. V., Stepanov, D. L., Stepanova, G, A., Shostakova, M.F., and Einor, O, L., eds., *Paleontological atlas of Carboniferous strata in the Urals*. Nedra, Leningrad, 154–258 (in Russian).

Scotese, C, R., 2004, A continental drift flipbook. *J. Geol.*, **112**, 729–741.

Sowerby, J., 1822, *The Mineral Conchology of Great Britain, vol. 4*, W. Ardling, London, 160 p.

Stehli, F. G., 1954, Lower Leonardian Brachiopoda of the Sierra Diablo. *Bull. Amer. Mus. Natur. Hist.*, **105**, 257–358.

Tan, Z., 1987, Brachiopoda. *In* Regional Geological Survey Party, Hunan Bureau of Geology and Mineral Resources, ed., *Late Devonian and Early Carboniferous stratigraphy and paleontology of Funan*. Geol. Pub. House, Beijing, 111–133 (in Chinese).

Tazawa, J., 2004, The strike slip model: A synthesis on the origin and tectonic evolution of the Japanese Islands. *Jour. Geol. Soc. Japan*, **110**, 503–517 (in Japanese).

Tazawa, J., 2018, Early Carboniferous (Mississippian) brachiopods from the Hikoroichi Formation, South Kitakami Belt, Japan. *Mem. Fukui Pref. Dinosaur Mus.*, **17**, 27–87.

Tazawa, J. and Ibaraki, Y., 2009, *Linoprotonia* and *Gigantoproductus* (Linoproductoidea, Brachiopoda) from the Lower Carboniferous in the Onimaru quarry, Hikoroichi, southern Kitakami Mountains, NE Japan. *Sci. Rep. Niigata Univ., (Geol.)*, no. 24, 7–19.

Tazawa, J. and Kato, M., 1986, *Striatifera* and *Gigantoproductus* from the Lower Carboniferous of Fukuji, Central Japan. *Trans. Proc. Palaeont. Soc. Japan, N. S.* no. 142, 393–399.

Tazawa, J., and Miyake, Y., 2002, *Gigantoproductus* (Brachiopoda) from the Lower Carboniferous (Upper Visean) Onimaru Formation of the southern Kitakami Mountains, NE Japan. *Sci. Rep. Niigata Univ., Ser. E*, no. 17, 1–6.

Tazawa, J., Sato, K. and Takenouchi, K., 2005, *Delepinea* and *Daviesiella* (Chonetoidea, Brachiopoda) from the Lower Carboniferous of Omi, central Japan. *Sci. Rep. Niigata Univ. (Geol.)*, no. 20, 1–13.

Tazawa, J., and Taira, M., 2020, Early Carboniferous (late Visean) brachiopods from the Onimaru Formation in the Nagaiwa-Onimaru area, South Kitakami Belt, northeastern Japan. *Sci. Rep. Niigata Univ., (Geol.)*, no. 35, 13–31.

Waagen, W., 1883, Salt Range fossils, 1. Productus-Limestone fossils: Brachiopoda. *Palaeont. Indica, Ser. 13*, **1**, 391–546.

Wang, S., 1984, Phylum Brachiopoda. *In* Regional Geological Surveying Team of Hubei, ed., *The Palaeontological Atlas of Hubei Province*. Hubei Sci. Tech. Press, Wuhan, 128–236 (in Chinese).

Wang, G., Liu, Q., Jing, Y., Hu, S., Liang, W. and Liao, Z., 1982, Brachiopoda. *In* Nanjin Institute of Geology and Mineral Resources, eds., *Paleontological Atlas of East China (Late Paleozoic)*, **2**, Geol. Pub. House, Beijing, 186–256 (in Chinese).

Yanagida, J., 1979, The large Carboniferous strophomenides from the Akiyoshi Limestone Group and their biostratigraphic significance. *Proc. Japan Acad., Ser. B*, **55**, 109–114.

Yanagida, J., 1989, Carboniferous brachiopods from the Akiyoshi Limestone Group, Southwest Japan. *In* Jin, Y. and Chun, L., eds., *11th Congr. Internat. Strat. Geol. Carbonifere Beijing 1987, Compte Rendu*, **2**, Nanjing Univ. Press, Nanjing. 391–398.

Yang, Z., Ding, P., Yin, H., Zhabg, S. and Fang, J., 1962, Carboniferous, Permian and Triassic brachiopod faunas from the Chilianshan region. *In* Chinese Institute of Geology and Palaeontology, Chinese Academy of Sciences, Institute of Geology, Chinese Academy of Sciences, Beijin Institute of Geology, eds., *Monogr. Geol. Chilianshan Mountains*, **4**, Sci. Pub. House, Beijing, 129 p. (in Chinese).

Yang, S., and Jiang. J., 1987, Early Carboniferous strata and brachiopods of Longmenshan Region, Sichuan. *In* Bureau of Geology and Mineral Resources of Guizhou Province Commission on Stratigraphy and Palaeontology, Geol. Soc. Guizhou Province, eds., *National Carboniferous Symposium of China, special paper*, Geol. Pub. House, Beijing, 69–92 (in Chinese).

Yang, D., Ni, S., Chang, M. and Zhao, R., 1977, Brachiopoda. *In* Hubei Institute of Geological Sciences and others, eds., *Paleontological Atlas of Central-South China, Late Paleozoic Part* 2, Geol. Pub. House, Beijing, 303–470 (in Chinese).

Zakowa, H., 1986, Brachiopods of the family Semiplanidae Sarycheva, 1960 from the Upper Visean of Poland. *Biul. Inst. Geol.*, no. 355, 49–70.

CONTENTS

8050 Ikarashi Nino-cho, Nishi-ku, Niigata 950-2181, Japan
TEL +81-(0)25-262-6197 FAX +81-(0)25-262-6194